

# 1 Evaluation of near surface ozone over Europe from the 2 MACC reanalysis

3 E. Katragkou<sup>1</sup>, P. Zanis<sup>1</sup>, A. Tsikerdekis<sup>1</sup>, J. Kapsomenakis<sup>2</sup>, D. Melas<sup>3</sup>, H.  
4 Eskes<sup>4</sup>, J. Flemming<sup>5</sup>, V. Huijnen<sup>4</sup>, A. Inness<sup>5</sup>, M.G. Schultz<sup>6</sup>, O. Stein<sup>6</sup>, C.S.  
5 Zerefos<sup>2</sup>

6 [1]{Department of Meteorology and Climatology, School of Geology, Aristotle University of  
7 Thessaloniki, Thessaloniki, Greece}

8 [2] {Research Centre for Atmospheric Physics and Climatology, Academy of Athens, Athens,  
9 Greece}

10 [3]{Laboratory of Atmospheric Physics, School of Physics, Aristotle University of  
11 Thessaloniki, Thessaloniki, Greece}

12 [4]{KNMI, De Bilt, the Netherlands}

13 [5] {ECMWF, Reading, UK}

14 [6] {Forschungszentrum Jülich, Jülich, Germany}

15 Correspondence to: E. Katragkou (katragou@auth.gr)

## 16 Abstract

17 This work is an extended evaluation of near surface ozone as part of the global reanalysis of  
18 atmospheric composition, produced within the European Funded project MACC (Monitoring  
19 Atmospheric Composition and Climate). It includes an evaluation over the period 2003-2012  
20 and provides an overall assessment of the modelling system performance with respect to near  
21 surface ozone for specific European subregions. Measurements at rural locations from the  
22 European Monitoring and Evaluation Program (EMEP) and the European Air Quality  
23 Database (AirBase) were used for the evaluation assessment. The fractional gross error of  
24 near surface ozone reanalysis is on average 24% over Europe, the highest found over  
25 Scandinavia (27%) and the lowest over the Mediterranean marine stations (21%). Near  
26 surface ozone shows mostly a negative bias in winter and a positive bias during warm months.  
27 Assimilation reduces the bias in near surface ozone in most of the European subregions -  
28 with the exception of the British Isles and the Iberian Peninsula and its impact is mostly  
29 notable in winter. With respect to the seasonal cycle, the MACC reanalysis reproduces the

1 photochemically driven broad spring-summer maximum of surface ozone of central and south  
2 Europe. However, it does not capture adequately the early spring peak and the shape of the  
3 seasonality at northern and north-eastern Europe. The diurnal range of surface ozone, which is  
4 as an indication of the local photochemical production processes, is reproduced fairly well,  
5 with a tendency for a small overestimation during the warm months for most subregions  
6 (especially in central and southern Europe). Possible reasons leading to discrepancies between  
7 the MACC reanalysis and observations are discussed.

## 8 **1 Introduction**

9 The European projects MACC (Monitoring Atmospheric Composition and Climate) and  
10 MACC-II (Interim Implementation) were established under the umbrella of the European  
11 Copernicus programme, formerly known as GMES (Global Monitoring for Environment and  
12 Security), to build and demonstrate a core capability for providing a comprehensive range of  
13 services related to the chemical and particulate composition of the atmosphere (Hollingsworth  
14 et al. 2008; Flemming et al., 2009; Inness et al., 2013). Within MACC operational forecasts of  
15 atmospheric composition on global (Stein et al., 2012) and regional scale are produced.  
16 Furthermore, the MACC reanalysis (Inness et al., 2013) provides global atmospheric  
17 composition fields which can be used to serve as boundary conditions for regional air quality  
18 models over Europe and world-wide.

19 The MACC global model used for both reanalysis and forecasts consists of the European  
20 Center for Medium-Range Weather Forecasts' (ECMWF) Integrated Forecast System (IFS)  
21 coupled to the MOZART-3 (Kinnison et al., 2007) chemistry transport model. The ECMWF  
22 modelling system makes use of its data-assimilation capabilities to combine observations of  
23 atmospheric composition with the numerical model in order to produce a reanalysis of  
24 atmospheric composition (Inness et al., 2009; Inness et al., 2015). ECMWF has many years of  
25 experience in producing reanalysis products, starting from ERA-40 (Dethof and Holm, 2004)  
26 and continuing with ERA-Interim (Dragani, 2010, 2011).

27 Evaluation of MACC data is being done on a regular basis (Eskes et al., 2015) and  
28 specifically for trace gases in the global troposphere (e.g. Stein et al., 2014) and the  
29 stratosphere (e.g. Lefever et al., 2014). The global reanalysis products are mostly used as a  
30 reference dataset for specific case studies (e.g. Knowland et al, 2014) or as boundary  
31 conditions for international activities, like the Air Quality Modelling Evaluation International  
32 Initiative-AQMEII (Air Quality Modelling Evaluation International Initiative) starting from

1 phase I (e.g. Schere et al., 2012) up to its current phase III. It is therefore useful to have a  
2 systematic analysis on a key atmospheric species of the global reanalysis product i) as a  
3 reference for those wishing to use it in their studies ii) as a general assessment of the system  
4 performance, identifying potential issues needing further improvement.

5 In this work special emphasis is given on the evaluation of near surface ozone over Europe for  
6 the whole reanalysis period produced within MACC (2003-2012). Near surface ozone is one  
7 of the main pollutants affecting both human health and vegetation (Fuhrer and Booker, 2003;  
8 Scebba et al., 2005; Schlink et al., 2006). Sources of tropospheric ozone can be either the  
9 stratosphere-troposphere transport or the photochemical production through oxidation of  
10 VOCs (volatile organic compounds) and CO in the presence of adequate NO<sub>x</sub>  
11 (NO<sub>x</sub>=NO<sub>2</sub>+NO) concentrations (Lelieveld and Dentener, 2000). Ozone can be destroyed  
12 photochemically or by dry deposition at the surface. Ozone precursors have natural as well as  
13 anthropogenic sources, the most important of which are emissions from soil, vegetation and  
14 fossil fuel combustion. Ambient ozone concentrations depend strongly on availability and  
15 relative abundance of those precursors but they are also modulated by the meteorological  
16 conditions (Davies et al., 1992; Bloomfield et al., 1996; Baertsch-Ritter et al., 2004; Hegarty  
17 et al., 2007; Kalabokas et al., 2008).

18 The issue of the short-term and long-term ozone variability is complex, being related to  
19 changes of anthropogenic and natural emissions, meteorological conditions, atmospheric  
20 boundary layer mixing processes and stratosphere-troposphere exchange. Although a number  
21 of measures aimed at reducing NO<sub>x</sub> and VOC emissions have been effective in reducing  
22 concentration of precursor species (Vestreng et al., 2009) and peak ozone values in Europe  
23 (EMEP/CCC-Report 1/2005;), there are many studies suggesting that background  
24 tropospheric ozone levels (even near the surface) are increasing (Chevalier et al., 2007;  
25 Ordóñez et al., 2007; Hess and Zbinden, 2013; Wilson et al., 2012; Akritidis et al., 2014).  
26 However, Parrish et al. (2012) reported a slower rate of increase over the last decades at  
27 European sites, to the extent that at present O<sub>3</sub> is decreasing at some sites, mostly in summer.

28 Furthermore, although the current consensus view is that photochemistry is the major  
29 contributor to the observed background ozone levels in the troposphere, there is still no  
30 consensus as to the mechanisms that lead to the formation of the spring ozone maximum  
31 observed in certain locations of the northern hemisphere, distant from nearby pollution  
32 sources (Crutzen et al., 1999; Lelieveld and Dentener, 2000; Monks, 2000; Zanis et al., 2007).

1 The spring ozone maximum observed in certain locations of the northern hemisphere, distant  
2 from nearby pollution sources, has mainly two contributions; i) the stratosphere to  
3 troposphere transport (STT) (Stohl et al., 2003 and references therein) and ii) ozone  
4 production in the troposphere on a hemispherical scale, related to photochemical processing  
5 of precursor tropospheric trace gases (CO, NO<sub>x</sub>, VOCs) built up in winter (Penkett and Brice,  
6 1987) and the longer lifetime of ozone during winter that allows anthropogenically produced  
7 ozone to accumulate (Lie et al., 1987; Yienger et al., 1999).

8 In this paper we evaluate near surface ozone of the MACC reanalysis over Europe from 2003  
9 to 2012. We provide an overall assessment of the model performance, putting special  
10 emphasis on the reproduction of annual and diurnal cycles. When possible, we provide  
11 potential explanations for model inabilities to reproduce specific observational characteristics  
12 of certain subregions and finally we suggest points of future work.

## 13 **2 Methodology**

### 14 **2.1 Global model**

15 The IFS includes greenhouse gases (Engelen et al., 2009) and aerosols (Benedetti et al., 2009;  
16 Morcrette et al., 2009). In MACC, the MOZART-3 chemistry transport model has been  
17 coupled to the IFS to provide chemical tendencies for ozone, carbon monoxide, nitrogen  
18 oxides, and formaldehyde (Flemming et al., 2009), while chemical data assimilation for these  
19 species takes place in IFS (Inness et al., 2009; Inness et al., 2015). MOZART-3 as used in the  
20 MACC reanalysis system is described in Stein et al. (2012; 2013).

21 A data assimilation system for aerosol, greenhouse gases and reactive gases is in place based  
22 on ECMWF's 4D-VAR data assimilation system. The fields of MACC reanalysis (hereafter  
23 MRE) are available globally at a horizontal resolution of ~80 km (T159 spectral resolution)  
24 and 60 hybrid sigma-pressure levels from the surface up to 0.1 hPa. More details on the CTM  
25 and the IFS configurations and the data assimilation system are provided by Inness et al.  
26 (2015) and references therein. A combination of profile and total column ozone retrievals was  
27 assimilated in MRE, namely GOME, MIPAS, MLS, OMI, SBUV/2, SCIAMCHY (Table 1)  
28 using ECMWF's 4D-Var assimilation algorithm (Courtier et al., 1994). For a more detailed  
29 description of the assimilation setup see Inness et al. (2013). It should be noted that no  
30 tropospheric ozone data were assimilated, so that the impact of the assimilation on near  
31 surface ozone comes from the residual of assimilating stratospheric and total column ozone.

1 More details on the impact of stratospheric ozone assimilation in tropospheric ozone is  
2 provided by Lefever et al. (2014).

3 Since several satellite instruments are used to assimilate one parameter in the data  
4 assimilation system, a bias correction method is applied to the data to account for the  
5 instrumental inconsistencies. In MRE a variational bias correction scheme for radiance data  
6 has been extended to atmospheric composition data (Inness et al., 2013). In the variational  
7 scheme biases are estimated during the analysis by including bias parameters in the control  
8 vector. The bias corrections are continuously adjusted to optimize the consistency with all  
9 information used in the analysis. The impact of assimilation on near surface ozone is only the  
10 “residual” of correcting the stratospheric and total ozone column, plus the assimilation of  
11 other relevant gases that impact ozone chemistry (CO, NO<sub>2</sub>) (Inness et al., 2013). The impact  
12 of the assimilation of tropospheric NO<sub>2</sub> columns from the Ozone Monitoring Instrument  
13 (OMI) is small because of the short lifetime of NO<sub>2</sub> (Inness et al., 2015).

14 To investigate the impact of assimilation on key atmospheric species, a control run was also  
15 performed (hereafter CTRL), using the same reanalysis settings without assimilation. As  
16 explained in Inness et al. (2013) (section 2.5), it would have been computationally too  
17 expensive to produce a control analysis experiment that was identical to the MACC  
18 reanalysis, but did not actively assimilate observations of reactive gases. Instead, a  
19 MOZART-3 stand-alone run was carried out that applied the same settings (model code,  
20 resolution, emissions) as MOZART in the MACC reanalysis. The meteorological data for the  
21 stand-alone run were taken from the reanalysis, but the control run had free-running  
22 chemistry. The results from this control run can be used to detect the impact of the  
23 assimilation of greenhouse reactive gases observations in the MACC reanalysis. Since the  
24 meteorological input data were derived from interpolation of archived 6-hourly output from  
25 the MACC reanalysis, and not through hourly exchange as in the reanalysis, the stand-alone  
26 run was not a completely clean control run. However, these differences would be small. The  
27 comparison between the MRE and the CTRL is confined to the time period 2003-2010, when  
28 both time series are available.

## 29 **2.2 Observations**

30 Measurements from ground based European stations were used for the evaluation of modelled  
31 surface ozone, from the European Monitoring and Evaluation Programme (EMEP) and the

1 European Environment Agency databases (AirBase) covering the time period from 2003 to  
2 2012. The observations used for this evaluation are independent from the assimilated ones.  
3 EMEP is appropriate to evaluate coarse resolution simulations, as it is fitted to catch  
4 background air pollution patterns with stations at a considerable distance from source areas in  
5 rural or remote regions (Schaap et al., 2015). Only background rural stations have been used  
6 from the AirBase database for comparisons with the coarse resolution model surface ozone.  
7 These include stations class 1-3 according to the Joly-Peuch classification methodology for  
8 surface ozone (Joly and Peuch, 2012). There is a total of 138 stations included in the current  
9 analysis, fulfilling the above-mentioned criteria. This selection ensures that all stations are  
10 adequate for comparisons with coarse resolution (80 km) model data.

11 Observed data from the EMEP and AirBase database were available in hourly resolution,  
12 while model values were available in 3-hourly intervals. The corresponding observational  
13 data were extracted with a 3-hourly interval, to be comparable with modelled time-series. The  
14 modelled data were extracted from the coupled system by means of interpolating surface  
15 ozone into each station location. Different model levels were used for comparison with  
16 ground based stations. The rationale behind the selection of different model level selection  
17 instead of extracting time series from the first model level (surface) is that in coarse resolution  
18 grids, areas with anomalous terrain (e.g. mountainous areas) are represented with an average  
19 elevation, which is less than the actual station elevation. Based on the difference between the  
20 actual station altitude and the average grid-cell elevation, the corresponding model level is  
21 selected, using atmospheric pressure as the correction criterion. We have used only those  
22 stations that fulfil the criteria of 75% data availability for near surface ozone.

23 In order to acquire a more detailed view of model performance, eight European subregions  
24 have been defined as shown in Figure 1. These regions fit data coverage and avoid  
25 overlapping between each subregion. The eight European subregions are: the British Isles  
26 (BI), France (FR), Iberian Peninsula (IP), East Europe (EA), Middle Europe (ME),  
27 Mediterranean (MD), South Middle Europe (SME) and Scandinavia (SC). Furthermore, the  
28 Mediterranean region was further split into the continental part (MDC) and the marine part  
29 (MDm), according to their spatial location (coastal or interior continental), since each type of  
30 station has different characteristics.

31 Additional NO and NO<sub>2</sub> data are included in the analysis, in order to assess the potential of  
32 the photochemical ozone production. The NO and NO<sub>2</sub> were extracted from EMEP and

1 AirBase. Unfortunately the number of EMEP stations that provide NO and NO<sub>2</sub>  
2 measurements – besides ozone – for the whole reanalysis period (2003-2012) is limited (30  
3 stations). After application of the station type classification for ozone and the data availability  
4 criteria, only 3 subregions with both O<sub>3</sub> and NO<sub>x</sub> measurements remained, namely the British  
5 Isles (BI) with 10 stations, Iberian Peninsula (IP) with 8 stations and Middle Europe (ME)  
6 with 12 stations. The plots referring to ozone and nitrogen-species comparison correspond to  
7 a smaller number of the common stations mentioned above, always being a subset of the total.

8 We have also to take into consideration that the NO<sub>x</sub> observations are affected strongly by  
9 local emissions. Furthermore there are known issues with interference by oxidized nitrogen  
10 compounds (e.g. HNO<sub>3</sub>, PAN and other organic nitrates) for ground-based NO<sub>2</sub>  
11 measurements by most commercially available NO<sub>2</sub> instruments using molybdenum  
12 converters, hence leading to an overestimation of NO<sub>x</sub> concentrations (Steinbacher et al.,  
13 2007).

14 Ozonesondes are used to validate ozone MRE profiles into the troposphere at 6 European  
15 stations: Haute-Provence (43.9N, 5.7E), Hohenpeissenberg (47.8N, 11E), Legionowo (52.4N,  
16 20.9E), Payerne (46.8N, 6.9E), Sodankyla (67.4N, 26.6E) and Uccle (50.8N, 4.3E). The  
17 sondes used for the validation come from Network for the Detection of Atmospheric  
18 Composition Change (NDACC; <ftp://ftp.cpc.ncep.noaa.gov/ndacc/station>). The precision of  
19 electrochemical concentration cell ozonesondes in the troposphere is between -7% and +17%  
20 below 200 hPa (Komhyr et al., 1995).

### 21 **2.3 Metrics and intercomparison methodology**

22 For the current evaluation study we use statistical metrics to quantify the bias, gross error and  
23 temporal correlation of the model with regards to observational surface ozone. Comparisons  
24 of the diurnal ranges and cycles are also performed, as indices of photochemical processes. As  
25 is also discussed by Savage et al. (2013), spatial and temporal variations in chemical  
26 composition, including tropospheric ozone, can be large, while also differences between  
27 model and observed values are frequently much larger in magnitude than usual for  
28 meteorological variables. Therefore, mean error and root mean square error, even though  
29 being important metrics for estimating model errors, are not optimal when assessing model  
30 performance at different chemical regimes as found over Europe.

1 Based on the evaluation guidelines and previous work within GEMS/MACC (Seigneur et al.,  
 2 2010; Elguindi et al., 2010; Ordonez et al., 2010; Eskes et al., 2015) we use the Modified  
 3 Normalized Mean Bias (MNMB) as a measure of the bias of modelled versus observed  
 4 values. This metric treats over- and underprediction in a symmetric manner ranging between -  
 5 2 and 2, in contrast to normalized mean bias that can grow to very high values much greater  
 6 than unit. The MNMB is calculated from equation (1) as follows:

$$7 \quad MNMB = \frac{2}{N} \sum_i^N \frac{f_i - o_i}{f_i + o_i} \quad (1)$$

8 where  $f_i$  and  $o_i$  are the mean monthly modelled and observed values, respectively and  $N$  the  
 9 sample size. Seasonal averages are calculated as: winter (DJF), spring (MAM), summer (JJA)  
 10 and autumn (SON).

11 Furthermore as a measure of the overall model error we use the Fractional Gross Error (FGE)  
 12 calculated from equation (2), with its values ranging between 0 and 2. The advantage of this  
 13 measure is the linear dependence on the departure, which makes this measure less sensitive to  
 14 outliers and tails in the distribution as compared to the more standard root-mean square.

$$15 \quad FGE = \frac{2}{N} \sum_i^N \left| \frac{f_i - o_i}{f_i + o_i} \right| \quad (2)$$

16 The Pearson correlation (R) is used for the quantification of the temporal agreement  
 17 (interannual variability), between the mean monthly observational and simulated data, where  
 18  $\sigma_f$  and  $\sigma_o$  in equation (3) denote the standard deviation of the modelled and observed values,  
 19 respectively:

$$20 \quad R = \frac{\frac{1}{N} \sum_i (f_i - \bar{f})(o_i - \bar{o})}{\sigma_f \sigma_o} \quad (3)$$

21 The annual cycle of the diurnal range was calculated from the mean diurnal cycle of each  
 22 station. The confidence interval for each month was derived using the values of the diurnal  
 23 range for the stations that reside in the same subregion.

24 In the following section we present a thorough evaluation of surface ozone covering the years  
 25 from 2003 to 2012, including the three basic validation metrics, analysis of diurnal/annual  
 26 cycles and diurnal ranges. Seasonal averages are calculated as: winter (DJF), spring (MAM),  
 27 summer (JJA) and autumn (SON). Additionally, surface ozone data are discussed along with



1 nitrogen oxides, wherever data allows comparisons, in order to characterize different  
2 chemistry regimes above Europe, with respect to photochemical production.

### 3 **3 Evaluation of the 2003-2012 MACC reanalysis near surface ozone**

#### 4 **3.1 Validation metrics**

5 The annual statistics of surface ozone are shown in Table 2. The FGE for the whole reanalysis  
6 period (2003-2012) ranges mostly from 21% in Mediterranean marine stations to 27% in  
7 Scandinavia. Figure 2 shows the basic validation metrics on a seasonal basis for the MACC  
8 reanalysis. Iberian Peninsula and Mid-Europe have a more stable performance with respect to  
9 FGE, with an average 20% for all seasons. All other regions have errors ranging from 10 to  
10 30% depending on season. A more thorough analysis on the seasonal behavior of surface  
11 ozone is provided in the following section.

12 The seasonal MNMB in Fig. 2 (middle panel) is close to zero for most subregions. The final  
13 MRE surface ozone product, exhibits its highest MNMB for Scandinavia and East Europe in  
14 winter (-20%). In summer the MNMB is mostly positive and remains  $\leq \pm 20\%$  for most sub-  
15 regions, with the exception of British Isles (+30%). Transitional season (spring/autumn)  
16 biases follow the patterns of the preceding season (winter/summer), since the atmospheric  
17 trace gases need some time to adjust from the winter to the summer-time chemistry regime.

18 Figure 2 (bottom panel) shows the temporal correlation of the 2003-2012 near-surface ozone  
19 timeseries, build upon mean monthly values, and therefore providing a clue on the  
20 representation of ozone seasonality. The lowest correlation is found over Scandinavia (0.26),  
21 followed by the British Isles (0.51) and the Mediterranean marine stations (0.54). All other  
22 regions have correlations  $\geq 0.7$ .

23 To investigate the impact of assimilation on near surface ozone we compare the MRE and  
24 CTRL simulations with the observations. Table 3 shows the annual statistics of the MRE and  
25 the CTRL simulation. The greatest improvement in the MACC reanalysis because of the  
26 assimilation is noted over Scandinavia, where the annual FGE is reduced from 40% to 27%,  
27 East Europe (FGE drops from 38% to 25%), Mediterranean continental stations (from 43% to  
28 29%) and Mid Europe (from 31% to 24%). In the same areas the MNMB is also reduced by  
29 up to 23% (SC). In France and the Iberian Peninsula there seems to be a small increase in the  
30 FGE (6 and 8% respectively) and a small change in the MNMB (reduced to zero in FR and

1 increased by 5% in IP). Over South Mid-Europe and the Mediterranean marine stations the  
2 change in FGE and MNMB is negligible on an annual basis.

3 The temporal correlation of monthly mean timeseries from 2003 to 2010 is reduced in the  
4 MRE, especially over the Mediterranean marine stations (drops from 0.74 to 0.49) and  
5 Scandinavia (from 0.39 to 0.23). The temporal correlation over Scandinavia is very low,  
6 because the MRE cannot capture the spring maximum, as it will be shown in section 3.2.  
7 Moreover, the issue of the MLS bias correction in the assimilation procedure has caused drifts  
8 in the tropospheric ozone concentrations between August 2004 and December 2007 (a  
9 detailed explanation of this issue can be found in Inness et al., 2013). The problem was  
10 tracked down and alleviated after year 2008 of the MRE. The deterioration of the temporal  
11 correlation in the MRE in comparison to the control simulation can be attributed to the  
12 assimilation procedure followed up to MRE year 2008. Calculation of temporal correlation  
13 coefficients before (2003-2007) and after (2008-2012) indicates that R increases in all  
14 subregions after removal of MLS bias correction. Figure 3 shows the comparison of the  
15 seasonal FGE, MNMB and R for the MRE and the CTRL near surface ozone over the  
16 different European subregions for the common time period 2003-2010. On a seasonal basis  
17 the greatest improvement due to assimilation is seen during the winter months, when the  
18 CTRL suffers from the largest negative bias. The impact on surface ozone is smaller in  
19 summer, eventually because near surface ozone is largely controlled by photochemical  
20 processes.

21

22

### 23 **3.2 Annual cycle of near surface ozone**

24 The average 2003-2012 observed and MRE annual cycle of near surface ozone is shown in  
25 Figure 4. With the only exception of the Mediterranean region (MDc and MDm), the modeled  
26 annual cycles of ozone have differences in the shape from the observed ones. The most  
27 striking disagreement is seen over Scandinavia (SC), where the MRE captures the annual  
28 range (13 ppb: the monthly maximum minus the monthly minimum of the year), but  
29 completely fails to reproduce surface ozone seasonality. While observations indicate a clear  
30 spring maximum (40 ppb), a characteristic ozone behavior in very clean and remote  
31 atmospheres in the northern hemisphere (Volz and Kley, 1988), no indication of spring ozone

1 maximum is evident in the MRE surface ozone; on the contrary, a clear lower maximum (35  
2 ppb) is found in late summer.

3 Over the British Isles (BI) we also note striking differences in the shape of the annual cycle.  
4 Specifically, there is disagreement a) in the “timeliness” of the early spring maximum, which  
5 is seen in April for observed ozone and the late spring-early summer for the MRE, and b) in  
6 the annual ozone range, which is overestimated by about 7 ppb. The overestimation occurs  
7 mainly during the summer/autumn season. We should note that, even though the MRE near  
8 surface ozone at SC and BI does not capture the observed spring maximum peaking in April,  
9 this spring ozone maximum is better seen in the lower free troposphere at 850 hPa and 700  
10 hPa vertical levels of MRE (not shown here).

11 In Mid-Europe (ME), the observational broad spring-summer maximum (April – July) is  
12 captured by the MRE, with a month’s time-lag (May to August) causing an underestimation  
13 in MRE of 2-3 ppbv from January to April and an overestimation from May to November  
14 (Fig 4). The highest overestimation (ranging from 5 ppbv to 9 ppbv) in MRE is seen during  
15 the warm months from June to September. This behavior results in an overestimated annual  
16 amplitude in MRE in comparison to observations.

17 Over the Iberian Peninsula (IP) there is an agreement in the seasonal cycle of MRE near  
18 surface ozone with observations, with a broad spring-summer maximum but MRE misses the  
19 April peak shown in observations. The amplitude of the MRE annual cycle is also  
20 overestimated by roughly 4 ppbv in comparison to observations, mostly stemming from the  
21 MRE summer O<sub>3</sub> overestimation, with the MRE June-maximum reaching up to 50 ppbv,  
22 while the observed to 40 ppbv. We should also take into consideration that the seasonal cycle  
23 of MRE at 700 hPa shows a broad spring-summer maximum with a peak in April as in near  
24 surface observations (discussed in Section 4.1).

25 A similar pattern of differences between MRE and observations are found for France (FR),  
26 South Mid-Europe (SME) and Eastern Europe (EA) although over EA the differences are  
27 smaller.

28 Overall, the annual cycles of the observed data reflect the specific subregional characteristics,  
29 namely the broad spring-summer maximum at Mediterranean (MDc and MDm) and South  
30 Mid-Europe (SME), the broad spring-summer maximum peaking in April at Eastern Europe  
31 (EA), Mid-Europe (ME), France (FR) and Iberian Peninsula (IP) and the early spring  
32 maximum over northern latitudes at Scandinavia (SC) and British Isles (BI). MRE near

1 surface ozone reproduces fairly well the photochemically driven broad spring-summer  
2 maximum of surface ozone of the sub-regions at central and south Europe, however, fails to  
3 capture the early spring peak in most of these subregions. This shortfall of MRE to capture  
4 the early spring peak has been also noted by Inness et al. (2013) and it is further discussed in  
5 the following sections. Furthermore, there is generally a tendency for overestimating the  
6 annual amplitude in MRE in comparison to observations.

7 Factors improving ozone seasonality could be emission strengths and temporal profiles and  
8 dry deposition (Val Martin et al., 2014). Ongoing work on the impact of dry deposition on  
9 surface ozone indicates that the new on-line dry depositions schemes currently tested in the C-  
10 IFS system improve the surface ozone positive bias, appearing mostly over southern Europe  
11 in summer, but cannot completely tackle the spring ozone maximum problem over north  
12 Europe (J. Flemming, personal communication, 2015).

### 13 **3.3 Diurnal cycle of near surface ozone**

14 Figure 5 depicts the mean 2003-2012 diurnal cycle of near surface ozone for each season for  
15 the selected European regions. All diurnal cycles have the expected behavior with sharply  
16 increasing ozone concentrations during the daytime hours (from 5:00-6:00 UTC in summer  
17 and 1-2 hours later in winter to 15:00-16:00 UTC) and decreasing afterwards. The diurnal  
18 cycles are more pronounced in the summer season and south Europe due to the more intense  
19 photochemistry. The MRE reproduces the diurnal cycle but exhibits positive bias in summer  
20 (except for the Mediterranean marine region), which may be persisting during the whole day  
21 (BI, SME, IP, ME) or occur mostly during daytime (EA, FR, MDc). In winter there is small  
22 negative bias in all regions, except for MDc (positive bias) and BI (zero bias). The transitional  
23 seasons have diurnal cycles that share both winter and summertime characteristics: the spring  
24 diurnal bias resembles winter with respect to bias, but has the enhanced photochemical  
25 diurnal cycle of summer, though not fully developed.

26 Figure 6 shows the annual cycle of the diurnal range of near surface ozone over the different  
27 European subregions. The diurnal range of ozone is a good indication of the potential for the  
28 local diurnal ozone build up through photochemical production processes (Zanis et al., 2000).  
29 There is generally a good agreement with observations, suggesting that MRE reproduces  
30 adequately the observed diurnal ozone range with a tendency for a small overestimation  
31 during the warm months for the subregions of central and south Europe. More specifically,

1 over SME, FR and MDc the diurnal range is overestimated during the whole year but, to a  
2 lesser extent in colder months, while over EA, ME, BI and SC the overestimation is smaller  
3 and restricted during the summer. Hence the diurnal range is overestimated more at the  
4 southern regions (SME, FR and MDc) than at the northern regions (EA, ME, BI and SC) and  
5 more during the warm months than during the cold months.

## 6 **4 Discussion**

7 In this section we discuss possible reasons for the differences revealed in the shape of the  
8 annual cycle of near surface ozone between observations and MRE and the failure in MRE to  
9 capture the early spring peak in most of the subregions. We discuss possible contributions  
10 from the above mentioned processes based on the comparison of MRE ozone profiles with  
11 available ozonesonde measurements, as well as on NO<sub>x</sub> versus O<sub>3</sub> annual and diurnal cycles.

### 12 **4.1 Ozone profiles**

13 Comparison with ozonesonde measurements at different locations (Fig. 7) indicate that MRE  
14 ozone profiles reproduce the basic structure of the profile, overestimating in most cases ozone  
15 below the 850hPa. . We note positive and negative biases depending on the location and the  
16 altitude, but there is a tendency for a larger positive bias during summer and autumn for most  
17 locations below 850 hPa, while the % biases in the middle and upper troposphere are  
18 generally smaller. This is in agreement with the study of Inness et al. (2013), who, analyzing  
19 MACC reanalysis over the time period (2003-2010), reported a negative bias with respect to  
20 ozonesondes above 650 hPa and the largest positive bias below 800 hPa. It should be also  
21 considered that the range of the % biases in the troposphere are comparable with the  
22 respective precision of electrochemical concentration cell ozonesonde measurements.

23 Furthermore, the shape of the observed ozone annual cycle (based on the ozonesondes) in  
24 lower free troposphere at 700 hPa is reproduced rather well by the MRE (Fig. 8). The course  
25 of the annual cycle is also reproduced for the middle troposphere at 500 hPa (not shown here).  
26 Despite the biases, the reasonable reproduction of the shape of the observed ozone seasonal  
27 cycle by MRE in the middle and lower free troposphere is consistent with transport processes  
28 from the lower stratosphere and the upper troposphere as well as long-range transport being  
29 resolved adequately by the MRE.

## 1 **4.2 NO<sub>x</sub> versus O<sub>3</sub> annual and diurnal cycles**

2 According to the analysis of ozone profiles (see Section 4.1) we may assume that assimilation  
3 in MRE leads to a reasonable representation of the ozone annual cycles at the middle and  
4 upper troposphere, thus mediating for a realistic contribution of STT. It could be hence  
5 speculated that differences in the shape of the seasonal cycle of near surface ozone between  
6 observations and the MRE could be also linked to the potential of photochemical ozone  
7 production and the strength of the exchange between the lower free troposphere and the  
8 atmospheric boundary layer (ABL). Two tentative explanations could be provided on the  
9 mismatch between model and observations: a) inadequate seasonality/emission strengths in  
10 surface emissions of precursor species (some issues discussed in Stein et al., 2014) and b) a  
11 loose coupling of the free troposphere to the ABL, which would be responsible for the  
12 entrainment of the assimilated free tropospheric O<sub>3</sub> into the ABL.

13 In global scales nitrogen oxides (NO<sub>x</sub>) are the limiting precursors for O<sub>3</sub> production  
14 throughout most of the troposphere, and also directly influence the abundance of the hydroxyl  
15 radical concentration in the troposphere (e.g. Crutzen, 1988). At regional scale for rural  
16 environments with NO<sub>x</sub> values less than a few parts per billion by volume, O<sub>3</sub> formation is  
17 NO<sub>x</sub> limited (Liu et al., 1987) and therefore almost independent of hydrocarbon  
18 concentrations, depending of course on the ratio of reactivity-weighted VOC mixture to NO<sub>x</sub>,  
19 which may differ from region to region across Europe (Beekmann and Vautard, 2010).  
20 Emissions of NO<sub>x</sub> occur primarily as NO, followed by oxidation to NO<sub>2</sub> while O<sub>3</sub> is  
21 photochemically produced as NO<sub>x</sub> are consumed in favor of their atmospheric oxidation  
22 products NO<sub>z</sub> (Liu et al., 1987; Zanis et al., 2007). NO<sub>z</sub> comprises mostly of  
23 peroxyacetylnitrate (PAN) and nitric acid (HNO<sub>3</sub>), along with HNO<sub>4</sub>, N<sub>2</sub>O<sub>5</sub>, NO<sub>3</sub> and other  
24 Acyl-peroxy nitrates (APNs) and organic nitrates (Emmons et al., 1997). The lifetime of NO<sub>x</sub>  
25 before photochemical conversion to NO<sub>z</sub> is less than a day in summer at mid-latitudes (Logan,  
26 1983).

27 Here, in order to assess the potential of the photochemical ozone production related to NO<sub>x</sub>  
28 emissions, we have looked at the annual cycle of NO<sub>x</sub> versus the respective annual cycle of  
29 O<sub>3</sub>, as well as the summertime diurnal cycle of O<sub>3</sub> along with the diurnal cycle of NO<sub>x</sub> at the  
30 different sub-regions of our domain. As mention in Section 2.2, after our station-filtering only  
31 3 sub-regions remained, with a considerable number of stations having both O<sub>3</sub> and NO<sub>x</sub>  
32 measurements; the British Isles (BI), Iberian Peninsula (IP) and Mid-Europe (ME).

1 Figure 9 shows the annual cycle of O<sub>3</sub> and NO<sub>x</sub> for BI, IP and ME. At the BI the NO<sub>x</sub> levels  
2 are overestimated in MRE throughout the year by up to 2 ppbv in comparison to the  
3 observations while ozone is overestimated from May to November. The overestimation of  
4 NO<sub>x</sub> concentrations at BI may partially account for the positive ozone bias during the warm  
5 period of the year, through overestimated photochemical ozone production. At IP and ME,  
6 NO<sub>x</sub> levels are systematically underestimated in MRE throughout the year, and still ozone is  
7 overestimated in MRE – especially during the warm part of the year – despite the NO<sub>x</sub>  
8 underestimation.

9 Figure 10 shows the average diurnal cycle of O<sub>3</sub> and NO<sub>x</sub> during summer for BI, IP and ME.  
10 Discarding any biases in the level of O<sub>3</sub> and NO<sub>x</sub> concentrations, it is shown that O<sub>3</sub> builds up  
11 during the daytime, while NO<sub>x</sub> is consumed in both MRE and observations. This daytime NO<sub>x</sub>  
12 decrease can be attributed to chemical loss through oxidation to NO<sub>z</sub>. Nevertheless, diurnal  
13 meteorological patterns of wind speed and boundary layer height, that lead to higher dilution  
14 of primary pollutants at daytime than at nighttime, may also contribute to the diurnal pattern  
15 of NO<sub>x</sub> in Figure 10 (see Figure S1 in the supplementary material). This is supported by the  
16 fact that CO in MRE, which is a species with much longer chemical lifetime than NO<sub>x</sub>, has a  
17 similar diurnal pattern with NO<sub>x</sub>.

18 Based on the diurnal amplitudes of O<sub>3</sub> ( $\Delta O_3$  increased over the day) and NO<sub>x</sub> ( $\Delta NO_x$   
19 decreased over the day) shown in Figure 10, we have calculated the ratio  $\Delta O_3/\Delta NO_x$  values  
20 for both MRE and observations. The  $\Delta O_3/\Delta NO_x$  ratio values for near surface based on MRE  
21 are estimated roughly to 3 for BI, 3.5 for ME and 10 for IP. The respective  $\Delta O_3/\Delta NO_x$  values  
22 based on the observed diurnal amplitudes are roughly 10 for BI, 6 for ME and 10 for IP.  
23 Additionally, we have also estimated  $\Delta O_3/\Delta NO_x$  ratio values based on MRE at 925 hPa  
24 (above near surface but within the atmospheric boundary layer) being roughly 3.5 for BI, 3  
25 for ME and 4 for IP. These ratio values reflect the ozone production efficiency, if we assume  
26 that daytime NO<sub>x</sub> loss is through oxidation to NO<sub>z</sub>. In order to compare these  $\Delta O_3/\Delta NO_x$  ratio  
27 values with theoretical calculations of ozone production efficiency, a zero dimension box  
28 model with the CBIV chemical mechanism was implemented to calculate ozone production  
29 efficiencies for typical summer conditions using initial conditions for NO<sub>x</sub> and other gaseous  
30 species from MRE at BI, IP and ME. These box model calculations indicated that 3 to 4  
31 molecules of O<sub>3</sub> produced for every molecule of NO<sub>x</sub> oxidised at BI and ME and up to 5 at IP.  
32 The above values agree well with ozone production efficiency estimates from previous studies

1 for summer at rural semi-polluted sites with  $\text{NO}_x$  more than a few ppbv in Europe and US  
2 (Chin et al., 1994; Derwent and Davis, 1994; Rickard et al., 2002). The  $\Delta\text{O}_3/\Delta\text{NO}_x$  ratio  
3 values based on MRE are comparable with the box model calculated ozone production  
4 efficiency values.

5 The amplitude of the diurnal cycle of  $\text{NO}_x$  is much stronger in the MRE, than at observations  
6 for BI and ME, which indicates that in MRE we presumably have a more intense local  
7 oxidation from  $\text{NO}_x$  to  $\text{NO}_z$ . This more intense local oxidation from  $\text{NO}_x$  to  $\text{NO}_z$  at BI and  
8 ME can lead to higher local photochemical ozone production, which may account for the  
9 slightly higher amplitude of the diurnal cycle of  $\text{O}_3$  for the MRE than the observations (by  
10 roughly 2 ppbv at BI and 1 ppbv at ME) and partially for the generally higher  $\text{O}_3$  levels of the  
11 MRE compared to the observed. The differences in local photochemical ozone production at  
12 BI and ME versus IP are consistent with the chemical regime indicator analysis for near  
13 surface ozone over Europe by Beekmann and Vautard (2010), who defined three particular  
14 regions: a) the region in North-Western Europe with a pronounced VOC sensitive regime  
15 (1W–6 E, 50 N–53 N), b) the Mediterranean region (6W–20 E, 38 N–43 N) with an average  
16  $\text{NO}_x$  sensitive chemical regime and c) Northern-Eastern Germany (9 E–14E, 50 N–54 N)  
17 which is a transition region between both regimes. Comparing this chemical regime analysis  
18 with our selected sub-regions BI, ME and IP, we note that BI and ME sub-regions are a  
19 mixture of a VOC sensitive regime and a  $\text{NO}_x$  sensitive regime, while IP is a  $\text{NO}_x$  sensitive  
20 regime.

21 In the case of IP, the amplitude of the diurnal cycle of  $\text{NO}_x$  is similar for both observations  
22 and MRE, while the amplitude of the diurnal cycle of  $\text{O}_3$  is slightly underestimated in the  
23 MRE, indicating that local photochemical ozone production is captured adequately or slightly  
24 underestimated. Nevertheless, the ozone levels are generally overestimated for the MRE,  
25 implying other processes than local photochemistry as a reason for the positive bias.

26

## 27 **5 Summary and Conclusions**

28 In the current work we evaluate the MACC-II reanalysis (MRE) near surface ozone for the  
29 time period 2003-2012 using rural stations of the EMEP and AirBase monitoring networks.  
30 Overall, the evaluation of MRE near surface ozone with station based observations shows a  
31 negative bias in winter over northern Europe and generally positive bias during warm months.  
32 With respect to the seasonal cycle, MRE reproduces the photochemically driven broad spring-



1 summer maximum of near surface ozone at central and south Europe. However, it does not  
2 adequately capture the shape of the seasonality with a characteristic early spring maximum at  
3 northern and north-eastern Europe. The diurnal range of surface ozone, which is as an  
4 indication of the local photochemical production processes, is reproduced fairly well in the  
5 MACC reanalysis, with a tendency for a small overestimation during the warm months for the  
6 subregions of central and south Europe. Comparison of MRE ozone profiles with ozonesonde  
7 profiles revealed reasonable reproduction of the shape of the observed ozone seasonal cycle in  
8 the middle and lower free troposphere, despite the biases. This suggests that transport  
9 processes from the lower stratosphere and the upper troposphere are resolved acceptably by  
10 MRE with the aid of the assimilation.

11 More specifically, the characteristics of near surface ozone in the MACC reanalysis 2003-  
12 2012 can be summarized as follows for the different sub-regions:

13 a) At British Isles and Scandinavia, the observed near surface spring ozone  
14 maximum peaking in April is not reproduced by MRE. However, this spring ozone  
15 maximum is better seen in the lower free troposphere (at 850 hPa and 700 hPa)  
16 implying adequate vertical transport within the free troposphere, as was also  
17 indicated by the good comparison with ozonesonde data. The possibility insufficient  
18 entrainment and mixing from the lower free troposphere into the atmospheric  
19 boundary layer should be further investigated. MRE diurnal range of near surface  
20 ozone compares relatively well with the observed diurnal range with a slight  
21 overestimation during summer. Analysis of the average MRE diurnal cycle of O<sub>3</sub>  
22 versus NO<sub>x</sub> during summer for the BI could possibly indicate among other reasons,  
23 more intense local oxidation from NO<sub>x</sub> to NO<sub>z</sub> than the observed and a systematic  
24 positive bias in NO<sub>x</sub> which can lead to higher local photochemical ozone production.

25 b) The ozone summer maximum of the Mediterranean area is captured by the MRE,  
26 with a slight overestimation during summer and autumn for the continental stations  
27 (MDc). The MRE near surface ozone diurnal range compares well with the observed  
28 one throughout the year for the marine stations (MDm) and is slightly overestimated  
29 during the warm months for the continental stations (MDc). This implies that part of  
30 the MRE overestimation of near surface in summer and autumn for MDc may be  
31 associated to an overestimation of local photochemical production. Zanis et al.  
32 (2014) also noted for the Mediterranean an overestimation of near surface ozone

1 during summer by another global chemistry–climate model, due to overestimated  
2 photochemical ozone production within the atmospheric boundary layer.

3 c) In East Europe, Mid-Europe, South Mid-Europe and France, MRE near surface  
4 ozone reproduces the photochemically driven broad spring-summer maximum, but  
5 fails to capture the early spring peak in April. Furthermore, there is a slight shift of  
6 the seasonal cycle towards summer in MRE compared to observations, with a  
7 tendency for an underestimation of ozone levels in cold months (from January to  
8 April) and an overestimation in summer and autumn. The diurnal range of near  
9 surface ozone in the MRE is overestimated during summer. This maybe implies an  
10 overestimated local photochemical ozone production, which can partially account for  
11 the summer overestimated MRE near surface ozone levels (similarly to MDc).  
12 Further analysis of the average diurnal cycle of O<sub>3</sub> versus NO<sub>x</sub> during summer for  
13 Mid-Europe, gives some indication for more intense local oxidation from NO<sub>x</sub> to  
14 NO<sub>z</sub> for the MRE than the observations, which can lead to higher local  
15 photochemical ozone production despite the systematic negative bias in NO<sub>x</sub>.

16 d) At the Iberian Peninsula there is a positive bias throughout the year and the MRE  
17 does not capture the April peak shown in the observed seasonal cycle. The MRE  
18 diurnal range compares relatively well with the observed diurnal range, maybe  
19 indicating that local photochemical production is captured adequately throughout the  
20 year. This is also supported from the analysis of the average diurnal cycle of O<sub>3</sub>  
21 versus NO<sub>x</sub> during summer. The seasonal cycle of MRE at 700 hPa shows a broad  
22 spring-summer maximum with a peak in April as in near surface observations. This  
23 feature could possibly indicate a loose coupling of the free troposphere with  
24 atmospheric boundary layer.

25 Our analysis suggests that in order to understand better the behaviour of near surface ozone,  
26 further analysis is needed for firm conclusions, including model diagnostics for  
27 photochemical production and loss terms, as well as the mixing between ABL and free  
28 troposphere. Improvement in the dry-deposition scheme –which is fixed in the current  
29 implementation – would also contribute to improvement of model performance  
30 (bias/seasonality) with respect to near surface ozone.

### 31 **Acknowledgements**

1 MACC II is funded by the European Union's Seventh Framework Programme (FP7) under  
2 Grant Agreement no. 283576. We thank the European Environmental Agency (AirBase) and  
3 the European Monitoring and Evaluation Programme (EMEP) for providing access to  
4 European O<sub>3</sub> and NO<sub>x</sub> observations

## 5 **References**

- 6 Akritidis D., Zanis, P., Pytharoulis, I., Karacostas, Th.: Near-surface ozone trends over  
7 Europe in RegCM3/CAMx simulations for the time period 1996-2006, *Atmospheric*  
8 *Environment*, 97, 6-18, 2014.
- 9 Baertsch-Ritter, N., Keller, J., Dommen, J., and Prévôt, A. S. H.: Effects of various  
10 meteorological conditions and spatial emission resolutions on the ozone concentration and  
11 ROG/NO<sub>x</sub> limitation in the Milan area (I), *Atmos. Chem. Phys.*, 4, 423–438,  
12 doi:10.5194/acp-4-423-2004, 2004.
- 13 Bhartia, P. K. and Wellemeyer, C.: TOMS-V8 total O<sub>3</sub> algorithm, in: OMI Ozone Product  
14 ATBD Volume II, NASA Goddard Space Flight Center, Greenbelt, MD, USA, 2002.
- 15 Bhartia, P. K., McPeters, R. D., Mateer, C. L., Flynn, L. E., and Wellemeyer, C., Algorithm  
16 for the estimation of vertical ozone profiles from the backscattered ultraviolet technique,  
17 *J. Geophys. Res.*, 101, 18793–18806, 1996.
- 18 Beekmann, M. and Vautard, R.: A modelling study of photochemical regimes over Europe:  
19 robustness and variability, *Atmos. Chem. Phys.*, 10, 10067-10084, doi:10.5194/acp-10-  
20 10067-2010, 2010.
- 21 Benedetti, A., Morcrette, J.-J., Boucher, O., Dethof, A., Engelen, R. J., Fisher, M., Flentje, H.,  
22 Huneus, N., Jones, L., Kaiser, J. W., Kinne, S., Mangold, A., Razinger, M., Simmons, A.  
23 J., Suttie, M., and the GEMS-AER team: Aerosol analysis and forecast in the European  
24 Centre for Medium-Range Weather Forecasts Integrated Forecast System: 2. Data  
25 assimilation, *J. Geophys. Res.*, 114, D13205, doi:10.1029/2008JD011115, 2009.
- 26 P. J.: Tropospheric ozone: An overview, in: *Tropospheric Ozone*, edited by: I.S.A.  
27 Isaksen, D. Reidel Publ. Co., 3–32, 1988.
- 28 Bloomfield, P., Royle, J. A., Steinberg, L. J., and Yang, Q.: Accounting for meteorological  
29 effects in measuring urban ozone levels and trends, *Atmos. Environ.*, 30(17), 3067–3077,  
30 1996.
- 31 Carli, B., Alpaslan, D., Carlotti, M., Castelli, E., Ceccherini, S., Dinelli, B. M., Dudhia, A.,  
32 Flaud, J. M., Hopfner, M., Jay, V., Magnani, L., Oelhaf, H., Payne, V., Piccolo, C.,  
33 Prospero, M., Raspollini, P., Ridolfi, M., Remedios, J., and Spang, R.: First results from  
34 MIPAS/ENVISAT with operational level 2 code, *Adv. Space Res.*, 33, 1012–1019,

1 doi:10.1016/S0273-1177(03)00584-2, 2004. Chevalier, A., Gheusi, F., Delmas, R.,  
2 Ordonez, C., Sarrat, C., Zbinden, R., Thouret, V., Athier, G., Cousin, J.M.: Influence of  
3 altitude on ozone levels and variability in the lower troposphere: a ground-based study for  
4 western Europe over the period 2001-2004, *Atmos. Chem. Phys.* 7, 4311-4326, 2007.

5 Chin, M., Jacob, D. J., Munger, J. W., Parrish, D. D., and Doddridge, B. G.: Relationships of  
6 ozone and carbon monoxide over North America, *J. Geophys. Res.* 99, 14,565–14,573,  
7 1994.

8 Courtier, P., Thépaut, J.-N. and Hollingsworth, A.: A strategy for operational implementation  
9 of 4D-Var, using an incremental approach, *Q. J. Roy. Meteor. Soc.*, 120, 1367–1388,  
10 1994. Crutzen, P. J., Lawrence, M. G., and Poeschl, U.: On the background  
11 photochemistry of tropospheric ozone, *Tellus*, 51A-B, 123–146, 1999. Derwent, R. G. and  
12 Davis, T. J.: Modelling the impact of NO<sub>x</sub> or hydrocarbon control on photochemical  
13 ozone in Europe, *Atmos. Environ.* 28, 2039–2052, 1994.

14 Dethof, A. and Holm, E. V.: Ozone assimilation in the ERA-40 re-analysis project, *Q. J. Roy.*  
15 *Meteor. Soc.*, 130, 2851–2872, 2004.

16 Dragani, R.: On the quality of the ERA-Interim ozone reanalyses: comparisons with in situ  
17 data, ERA Report Series, 2, available at:  
18 <http://www.ecmwf.int/publications/library/do/references/list/782009> (last access: 29  
19 November 2012), 2010.

20 Dragani, R.: On the quality of the ERA-Interim ozone reanalyses: comparisons with satellite  
21 data, *Q. J. Roy. Meteor. Soc.*, 137, 1312–1326,  
22 doi:<http://dx.doi.org/10.1002/qj.82110.1002/qj.821>, 2011.

23 Elguindi, N., Clark, H., Ordóñez, C., Thouret, V., Flemming, J., Stein, O., Huijnen, V.,  
24 Moinat, P., Inness, A., Peuch, V.-H., Stohl, A., Turquety, S., Athier, G., Cammas, J.-P.,  
25 and Schultz, M.: Current status of the ability of the GEMS/MACC models to reproduce  
26 the tropospheric CO vertical distribution as measured by MOZAIC, *Geosci. Model Dev.*,  
27 3, 501-518, doi:10.5194/gmd-3-501-2010, 2010.

28 EMEP/CCC-Report 1/2005, March 2005. The development of European surface ozone.  
29 Implications for a revised abatement policy. In: Solberg, Sverre, Lindskog, Anne (Eds.), A  
30 Contribution from the EU Research Project NEPAP U-103003. Emmons, L. K., Carroll, M.  
31 A., Hauglustaine, D. A., Brasseur, G. P., et al.: Climatologies of NO<sub>x</sub> and NO<sub>y</sub>: A  
32 comparison of data and models, *Atmos. Environ.*, 31(12), 1851–1904, 1997.

1 Engelen, R. J., Serrar, S., and Chevallier, F.: Four-dimensional data assimilation of  
2 atmospheric CO<sub>2</sub> using AIRS observations, *J. Geophys. Res.*, 114, D03303,  
3 doi:10.1029/2008JD010739, 2009.

4 Eskes, H. J., van der A, R. J., Brinksma, E. J., Veeffkind, J. P., de Haan, J. F., and Valks, P. J.  
5 M.: Retrieval and validation of ozone columns derived from measurements of  
6 SCIAMACHY on Envisat, *Atmos. Chem. Phys. Discuss.*, 5, 4429– 4475,  
7 doi:10.5194/acpd-5-4429-2005, 2005.

8 Eskes H., V. Huijnen, A. Arola, A. Benedictow, A. Blechschmidt, E. Botek, O. Boucher, I.  
9 Bouarar, S. Chabrillat, E. Cuevas, R. Engelen, H. Flentje, A. Gaudel, J. Griesfeller, L.  
10 Jones, J. Kapsomenakis, E. Katragkou, S. Kinne, B. Langerock, M. Razinger, A. Richter,  
11 M. Schultz, M. Schulz, N. Sudarchikova, V. Thouret, M. Vrekoussis, A. Wagner, and C.  
12 Zerefos, Validation of reactive gases and aerosols in the MACC global analysis and  
13 forecast system, *Geosci. Model Dev. Discuss.*, 8, 1117-1169, 2015 Flemming, J., Dethof,  
14 A., Moinat, P., Ordonez, C., Peuch, V.-H., Segers, A., Schultz, M., Stein, O., van Weele,  
15 M.: Coupling global atmospheric chemistry transport models to ECMWF Integrated  
16 Forecasts System for forecast and data assimilation within GEMS, in: *Integrated Systems*  
17 *of Meso-Meteorological and Chemical Transport Models*, edited by: Baklanov, A.,  
18 Mahura, A., and Sokhi, R., Springer-Verlag, Berlin Heidelberg, doi:10.1007/978-3-642-  
19 13980-2 10, 2011. Fuhrer, J. and Booker, F.: Ecological issues related to ozone:  
20 agricultural issues, *Environ. Int.* 29(2–3), 141–154, 2003.

21 Flemming J., Inness, A. Flentje, H. Huijnen, V. Moinat, P. Schultz, M. G.. Stein, O.:  
22 Coupling global chemistry transport models to ECMWF’s integrated forecast system,  
23 *Geosci. Model Dev.*, 2, 253–265, doi:10.5194/gmd-2-253-2009, 2009.

24 Hegarty J., Mao, H., and Talbot, R.: Synoptic controls on summertime surface ozone in the  
25 northeastern United States, *J. Geophys. Res.*, 112, D14306, doi:10.1029/2006JD008170,  
26 2007.

27 Hess, P.G., Zbinden, R.: Stratospheric impact on tropospheric ozone variability and trends:  
28 1990e2009. *Atmos. Chem. Phys.* 13, 2013.

29 Hollingsworth, A., Engelen, R. J., Textor, C., Benedetti, A., Boucher, O., Chevallier, F.,  
30 Dethof, A., Elbern, H., Eskes, H., Flemming, J., Granier, C., Kaiser, J. W., Morcrette, J.-  
31 J., Rayner, P., Peuch, V. H., Rouil, L., Schultz, M. G., Simmons, A. J., and 5 The GEMS  
32 Consortium: toward a monitoring and forecasting system for atmospheric composition:  
33 the GEMS project, *B. Am. Meteorol. Soc.*, 89, 1147–1164, 2008.

1 Inness, A., Flemming, J., Suttie, M., and Jones, L.: GEMS data assimilation system for  
2 chemically reactive gases, European Centre for Medium-Range Weather Forecasts  
3 (ECMWF), Technical Memorandum No. 587, 2009.

4 Inness, A., Baier, F., Benedetti, A., Bouarar, I., Chabrillat, S., Clark, H., Clerbaux, C.,  
5 Coheur, P., Engelen, R. J., Errera, Q., Flemming, J., George, M., Granier, C., Hadji-  
6 Lazaro, J., Huijnen, V., Hurtmans, D., Jones, L., Kaiser, J. W., Kapsomenakis, J., Lefever,  
7 K., Leitão, J., Razinger, M., Richter, A., Schultz, M. G., Simmons, a. J., Suttie, M., Stein,  
8 O., Thépaut, J.-N., Thouret, V., Vrekoussis, M. and Zerefos, C.: The MACC reanalysis:  
9 an 8 yr data set of atmospheric composition, *Atmos. Chem. Phys.*, 13(8), 4073–4109,  
10 doi:10.5194/acp-13-4073-2013, 2013.

11 Inness, A., Blechschmidt, A., Bouarar, I., Chabrillat, S., Crepulja, M., Engelen, R. J., Errera,  
12 Q., Flemming, J., Gaudel, A., Huijnen, V., Jones, L., Kapsomenakis, J., Keppens, A.,  
13 Lambert, J.-C., Langerock, B., Peuch, V. H., Razinger, M., Richter, A., Schultz, M.  
14 G., Suttie, M., Thouret, V., Vrekoussis, M., Wagner, A., and Zerefos, C.: Data assimilation  
15 experiments of satellite retrievals of O<sub>3</sub>, CO and NO<sub>2</sub> with Composition IFS Atmos.  
16 *Chem. Phys.*, 15, 5275–5303, 2015

17 Joly, M. and Peuch, V.-H., Objective classification of air quality monitoring sites over Europe  
18 (2012), *Atmospheric Environment*, 47, pp. 111-123.

19 Kalabokas, P. D., Mihalopoulos, N., Ellul, R., Kleanthous, S., and Repapis, C. C.: An  
20 investigation of the meteorological and photochemical factors influencing the background  
21 rural and marine surface ozone levels in the Central and Eastern Mediterranean, *Atmos.*  
22 *Environ.*, 42, 7894–7906, doi:10.1016/j.atmosenv.2008.07.009, 2008.

23 Knowland K.E., R. M. Doherty, and K. I. Hodges, The effects of springtime mid-latitude  
24 storms on trace gas composition determined from the MACC reanalysis. *Atmos. Chem.*  
25 *Phys. Discuss.*, 14, 27093-27141, 2014

26 Komhyr, W. D., Barnes, R. A., Borthers, G. B., Lathrop, J. A., Kerr, J. B., and Opperman, D.  
27 P.: Electrochemical concentration cell ozonesonde performance evaluation during STOIC  
28 1989, *J. Geophys. Res.*, 100, 9231–9244, 1995.

29 Lefever K., R. van der A, F. Baier, Y. Christophe, Q. Errera, H. Eskes, J. Flemming, A.  
30 Inness, L. Jones, J.-C. Lambert, B. Langerock, M. G. Schultz, O. Stein, A. Wagner, and S.  
31 Chabrillat, Copernicus atmospheric service for stratospheric ozone: validation and  
32 intercomparison of four near real-time analyses, 2009–2012, *Atmos. Chem. Phys.*  
33 *Discuss.*, 14, 12461-12523, 2014

- 1 Lelieveld, J. and Dentener, F.: What controls tropospheric ozone, *J. Geophys. Res.*, 105(3),  
2 3543–3563, 2000.
- 3 Levelt, P. F., van den Oord, G. H. J., Dobber, M. R., Mäkelä, A., Visser, H., de Vries, J.,  
4 Stammes, P., Lundell, J. O. V., and Saari, H.: The ozone monitoring instrument, *IEEE T.*  
5 *Geosci. Remote*, 44, 1093–1101, 2006.
- 6 Liu, S. C., Trainer, M., Fehsenfeld, F. C., Parrish, D. D., Williams, E. J., Fahey, D. W.,  
7 Hübler, G., and Murphy, P. C.: Ozone Production in the Rural Troposphere and the  
8 Implications for Regional and Global Ozone Distributions, *J. Geophys. Res.*, 92(D4),  
9 4191–4207, 1987.
- 10 Monks, P. S.: A review of observations and origins of the spring ozone maximum, *Atmos.*  
11 *Environ.*, 34, 3545–3561, 2000.
- 12 Morcrette, J.-J., Boucher, O., Jones, L., Salmond, D., Bechtold, P., Beljaars, A., Benedetti, A.,  
13 Bonet, A., Kaiser, J.W., Razinger, M., Schulz, M., Serrar, S., Simmons, A.J., Sofiev, M.,  
14 Suttie, M., Tompkins, A.M., Untch, A., Aerosol analysis and forecast in the european  
15 centre for medium-range weather forecasts integrated forecast system: Forward modeling  
16 (2009) *Journal of Geophysical Research: Atmospheres*, 114 (6)
- 17 Ordóñez, C., Brunner, D., Staehelin, J., Hadjinicolaou, P., Pyle, J.A., Jonas, M., Wernli, H.,  
18 Prevot, A.S.H.: Strong influence of lowermost stratospheric ozone on lower tropospheric  
19 background ozone changes over Europe. *Geophys. Res. Lett.* 34, L07805. , 2007.
- 20 Ordóñez C., N. Elguindi, O. Stein, V. Huijnen, J. Flemming, A. Inness, H. Flentje, E.  
21 Katragkou, P. Moinat, V-H. Peuch, A. Segers, V. Thouret, M. van Weele, C. S. Zerefos, J-  
22 P. Cammas, and M. G. Schultz, Global model simulations of air pollution during the 2003  
23 European heat wave, *Atmospheric Chemistry and Physics*, 10, 789–815, 2010
- 24 Parrish, D.D., Lamarque, J.-F., Naik, V., Horowitz, L., Shindell, D.T., Staehelin, J., Derwent,  
25 R., Cooper, O.R., Tanimoto, H., Volz-Thomas, A., Gilge, S., Scheel, H.-E., Steinbacher,  
26 M., Fröhlich, M., Long-term changes in lower tropospheric baseline ozone concentrations:  
27 Comparing chemistry-climate models and observations at northern midlatitudes (2014)  
28 *Journal of Geophysical Research: Atmospheres*, 119 (9), pp. 5719-5736.
- 29 Penkett, S. A. and Brice, K. A.: The spring maximum in photooxidant in the Northern  
30 hemisphere troposphere, *Nature*, 319, 655–657, 1986.
- 31 Rickard, A. R., Salisbury, G., Monks, P. S., Lewis, A. C., Baugitte, S., Bandy, B. J.,  
32 Clemitshaw, K. C., and Penkett, S. A.: Comparison of measured ozone production

1 efficiencies in the marine boundary layer at two European coastal sites under different  
2 pollution regimes, *J. Atmos. Chem.*, 43, 107–134, 2002.

3 Savage, N. H., Agnew, P., Davis, L. S., Ordóñez, C., Thorpe, R., Johnson, C. E., O'Connor, F.  
4 M., and Dalvi, M.: Air quality modelling using the Met Office Unified Model (AQUUM  
5 OS24-26): model description and initial evaluation, *Geosci. Model Dev.*, 6, 353-372,  
6 doi:10.5194/gmd-6-353-2013, 2013.

7 Siddans, R., Reburn, W. J., Kerridge, B. J., and Munro, R.: Height resolved ozone  
8 information in the troposphere and lower stratosphere stratosphere from GOME,  
9 Technical report, British Atmospheric Data Centre (BADC), available at:  
10 <http://cedadocs.badc.rl.ac.uk/97/> (last access: 29 November 2012), 2007.

11 Schaap, M., Cuvelier, C., Hendriks, C., Bessagnet, B., Baldasano, J.M., Colette, A., Thunis,  
12 P., Karam, D., Fagerli, H., Graff, A., Kranenburg, R., Nyiri, A., Pay, M.T., Rouïl, L.,  
13 Schulz, M., Simpson, D., Stern, R., Terrenoire, E., Wind, P., Performance of European  
14 chemistry transport models as function of horizontal resolution (2015) *Atmospheric*  
15 *Environment*, 112, pp. 90-105

16 Scebba, F., Giuntini, D., Castagna, A., Soldatini, G., and Ranieri, A.: Analysing the impact of  
17 ozone on biochemical and physiological variables in plant species belonging to natural  
18 ecosystems, *Environ. Exp. l Bot.*, 235–246, 2005.

19 Schere, K., Flemming, J., Vautard, R., Chemel, C., Colette, A., Hogrefe, C., Bessagnet, B.,  
20 Meleux, F., Mathur, R., Roselle, S., Hu, R.-M., Sokhi, R.S., Rao, S.T., Galmarini, S.  
21 Trace gas/aerosol boundary concentrations and their impacts on continental-scale  
22 AQMEII modeling domains (2012) *Atmospheric Environment*, 53, pp. 38-50.

23 Schlink U., Herbarth, O., Richter, M., Dorling, S., Nunnari, G., Cawley, G., and Pelikan, E.:  
24 Statistical models to assess the health effects and to forecast ground-level ozone, *Environ.*  
25 *Modell. Soft.*, 21(4), 547–558, 2006.

26 Stein, O.: Model documentation of the MOZART CTM as implemented in the GEMS system,  
27 available at: <http://gems.ecmwf.int/do/get/PublicDocuments/1531/1172> (last access: 29  
28 November 2012), 2009.

29 Stein, O., Flemming, J., Inness, A., Kaiser, J. W., and Schultz, M. G.: Global reactive gases  
30 forecasts and reanalysis in the MACC project, *J. Integr. Environ. Sci.*, 9, 57–70,  
31 doi:10.1080/1943815X.2012.696545, 2012.



- 1 Stein O., M. G. Schultz, I. Bouarar, H. Clark, V. Huijnen, A. Gaudel, M. George, and C.  
2 Clerbaux, On the wintertime low bias of Northern Hemisphere carbon monoxide found in  
3 global model simulations, *Atmos. Chem. Phys.*, 14, 9295–9316, 2014
- 4 Steinbacher, M., Zellweger, C., Schwarzenbach, B., Bugmann, S., Buchmann, B., Ordóñez, C.,  
5 Prevot, A. S. H., and Hueglin, C.: Nitrogen oxide measurements at rural sites in  
6 Switzerland: Bias of conventional measurement techniques, *J. Geophys. Res.*, 112,  
7 D11307, doi:10.1029/2006JD007971, 2007.
- 8 Stohl, A., Bonasoni, P., Cristofanelli, P., Collins, W., Feichter, J., Frank, A., Forster, C.,  
9 Gerasopoulos, E., Gäggeler, H., James, P., Kentarchos, T., Kreipl, S., Kromp-Kolb, H.,  
10 Krüger, B., Land, C., Meloen, J., Papayannis, A., Priller, A., Seibert, P., Sprenger, M.,  
11 Roelofs, G. J., Scheel, E., Schnabel, C., Siegmund, P., Tobler, L., Trickl, T., Wernli, H.,  
12 Wirth, V., Zanis, P., and Zerefos, C.: Stratosphere-troposphere exchange – a review, and  
13 what we have learned from STACCATO, *J. Geophys. Res.*, 108(D12),  
14 doi:10.1029/2002JD002490, 2003.
- 15 Valmartin, M., Heald, C.L., Arnold, S.R. Coupling dry deposition to vegetation phenology in  
16 the Community Earth System Model: Implications for the simulation of surface O<sub>3</sub> (2014)  
17 *Geophysical Research Letters*, 41 (8), pp. 2988-2996.
- 18 Valcke, S. and Redler, R.: OASIS4 User Guide (OASIS4 0 2), PRISM–Support Initiative,  
19 Technical Report No 4, available at: <http://www.prism.enes.org/Publications/index.php>  
20 (last access: 29 November 2012), 2006.
- 21 Vestreng, V., Ntziachristos, L., Semb, A., Reis, S., Isaksen, I.S.A., Tarrason, L.: Evolution of  
22 NO<sub>x</sub> emissions in Europe with focus on road transport control measures. *Atmos. Chem.*  
23 *Phys.* 9, 1503e1520, 2009.
- 24 Volz, A., Kley, D., Evaluation of the Montsouris series of ozone measurements made in the  
25 nineteenth century, *Nature*, 332 (6161), pp. 240-242, 1988
- 26 Waters, J.W., Froidevaux, L., Harwood, R. S., Jarnot, R. F., Pickett, H. M., Read, W. G.,  
27 Siegel, P. H., Cofield, R. E., Filipiak, M. J., Flower, D. A., Holden, J. R., Lau, G. K.,  
28 Livesey, N. J., Manney, G. L., Pumphrey, H. C., Santee, M. L., Wu, D. L., Cuddy, D. T.,  
29 Lay, R. R., Loo, M. S., Perun, V. S., Schwartz, M. J., Stek, P. C., Thurstans, R. P., Boyles,  
30 M. A., Chandra, K. M., Chavez, M. C., Chen, G.-S., Chudasama, B. V., Dodge, R., Fuller,  
31 R. A., Girard, M. A., Jiang, J. H., Jiang, Y., Knosp, B. W., LaBelle, R. C., Lam, J. C., Lee,  
32 K. A., Miller, D., Oswald, J. E., Patel, N. C., Pukala, D. M., Quintero, O., Scaff, D. M.,  
33 Van Snyder, W., Tope, M. C., Wagner, P. A., and Walch, M. J.: The Earth Observing  
34 System Microwave Limb Sounder (EOS MLS) on the Aura satellite, *IEEE Trans. Geosci.*  
35 *Remote*, 44, 1075–1092, 2006.

- 1 Wilson, R.C., Fleming, Z.L., Monks, P.S., Clain, G., Henne, S., Kononov, I.B., Szopa, S.,  
2 Menut, L.: Have primary emission reduction measures reduced ozone across Europe? An  
3 analysis of European rural background ozone trends 1996-2005. *Atmos. Chem. Phys.* 12,  
4 437e454. <http://dx.doi.org/10.5194/acp-12-437-2012>, 2012.
- 5 Yienger, J. J., Klonecki, A. A., Levy II, H., Moxim, W. J., and Carmichael, G. R.: An  
6 evaluation of chemistry's role in the winter-spring ozone maximum found in the northern  
7 midlatitude free troposphere, *J. Geophys. Res.*, 104(D3), 3655–3667, 1999.
- 8 Zanis P., P.S. Monks, E. Schuepbach, and S.A. Penkett, The role of in-situ photochemistry in  
9 the control of ozone during spring at the Jungfrauoch Observatory (3,580 m asl) –  
10 Comparison of model results with measurements, *Journal of Atmospheric Chemistry*,  
11 37(1), 1-27, 2000.
- 12 Zanis, P., Ganser, A., Zellweger, C., Henne, S., Steinbacher, M., and Staehelin, J.: Seasonal  
13 variability of measured ozone production efficiencies in the lower free troposphere of  
14 Central Europe, *Atmos. Chem. Phys.*, 7, 223–236, doi:10.5194/acp-7-223-2007, 2007.
- 15 Zanis P., P. Hadjinicolaou, A. Pozzer, E. Tyrllis, S. Dafka, N. Mihalopoulos, J. Lelieveld,  
16 Summertime free tropospheric ozone pool over the Eastern Mediterranean/Middle East,  
17 *Atmospheric Chemistry and Physics*, 14, 115–132, 2014.
- 18

1 Table 1: Ozone satellite retrievals that were assimilated in the MACC reanalysis. PROF  
2 denotes profile data, TC total columns, PC partial columns, and SOE solar elevation. PC  
3 SBUV/2 data consist of 6 layers between the surface and 0.1 hPa. NRT (near-real time) data  
4 are available within a few hours after the observation was made, and are being used in  
5 operational forecast systems. For periods towards the end of the MACC reanalysis period,  
6 NRT data were used for some of the species when no offline products were available.

Sensor	Satellite	Provider	Version	Period	Type	Data usage criteria	Reference
GOME	ERS-2	RAL		20030101- 20030531	O <sub>3</sub> PROF	Used if SOE>15° and 80°S<lat<80°N	Siddans et al. 2007
MIPAS	ENVISAT	ESA		20030127- 20040326	O <sub>3</sub> PROF	All data used	Carli et al. 2004
MLS	AURA	NASA	V02	20040808- 20090315,  NRT data from 20090316	O <sub>3</sub> PROF	All data used	Waters et al. 2006
OMI	AURA	NASA	V003	From 20041001, NRT data 20070321- 20071231	O <sub>3</sub> TC	Used if SOE >10°	Bhartia et al. 2002; Levelt et al. 2006
SBUV/2	NOAA-16	NOAA	V8	From 20040101	O <sub>3</sub> PC	Used if SOE>6°	Bhartia et al. 1996
SBUV/2	NOAA-17	NOAA	V8	From 20030101	O <sub>3</sub> PC	Used if SOE>6°	Bhartia et al. 1996
SBUV/2	NOAA-18	NOAA	V8	From 20050604	O <sub>3</sub> PC	Used if SOE>6°	Bhartia et al. 1996
SCIAMACHY	ENVISAT	KNMI		From 20030101	O <sub>3</sub> TC	Used if SOE>6°	Eskes et al. 2005

7

8

1 Table 2. Annual statistics of near surface ozone for the MACC reanalysis (2003-2012) over  
 2 the different European subregions. FGE and MNMB are expressed in %.

<b>Region</b>	<b>FGE</b>	<b>MNMB</b>	<b>R</b>
<b>BI</b>	23	12	0.51
<b>IP</b>	25	14	0.72
<b>FR</b>	26	-2	0.73
<b>ME</b>	22	3	0.74
<b>SC</b>	27	-13	0.26
<b>SME</b>	24	2	0.74
<b>MD<sub>c</sub></b>	24	20	0.71
<b>MD<sub>m</sub></b>	21	-12	0.54
<b>EA</b>	25	-9	0.66

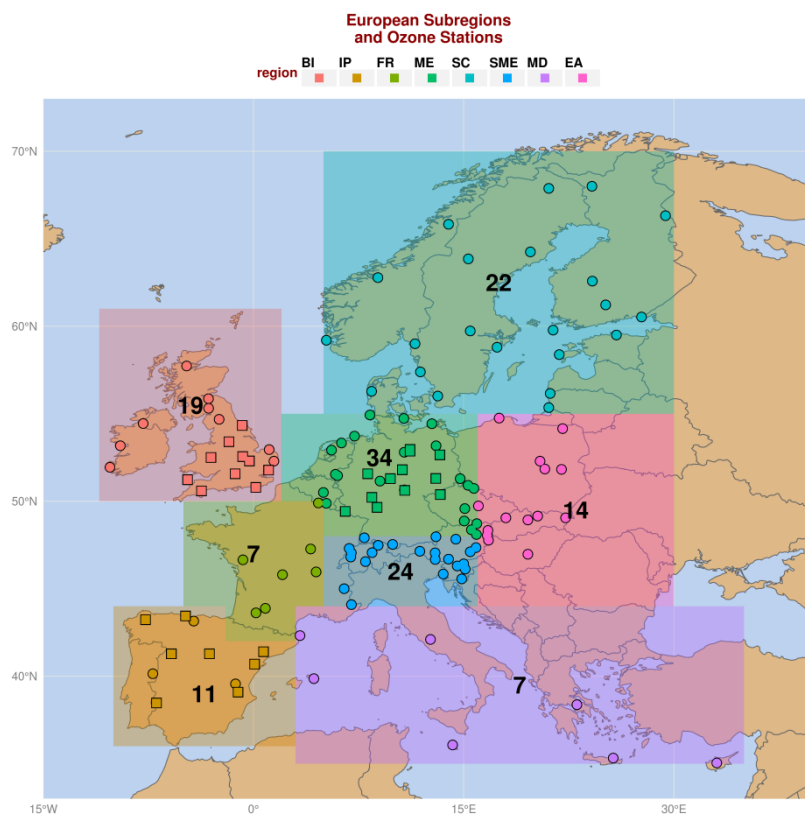
3

4 Table 3. Annual statistics of near surface ozone for the MACC reanalysis (MRE) and the  
 5 control run (CTRL) over the different European subregions for the common period from  
 6 2003 to 2010. FGE and MNMB are expressed in %.

7

<b>Region</b>	<b>FGE</b>		<b>MNMB</b>		<b>R</b>	
	<b>MRE</b>	<b>CTRL</b>	<b>MRE</b>	<b>CTRL</b>	<b>MRE</b>	<b>CTRL</b>
<b>BI</b>	24	22	13	-7	0.51	0.59
<b>IP</b>	25	17	15	10	0.70	0.79
<b>FR</b>	28	22	0	-5	0.73	0.79
<b>ME</b>	24	31	4	-17	0.73	0.80
<b>SC</b>	27	40	-12	-35	0.23	0.39
<b>SME</b>	25	22	3	-5	0.73	0.78
<b>MD<sub>c</sub></b>	29	43	26	42	0.71	0.74
<b>MD<sub>m</sub></b>	21	19	-10	-12	0.49	0.74
<b>EA</b>	25	38	-8	-28	0.64	0.70

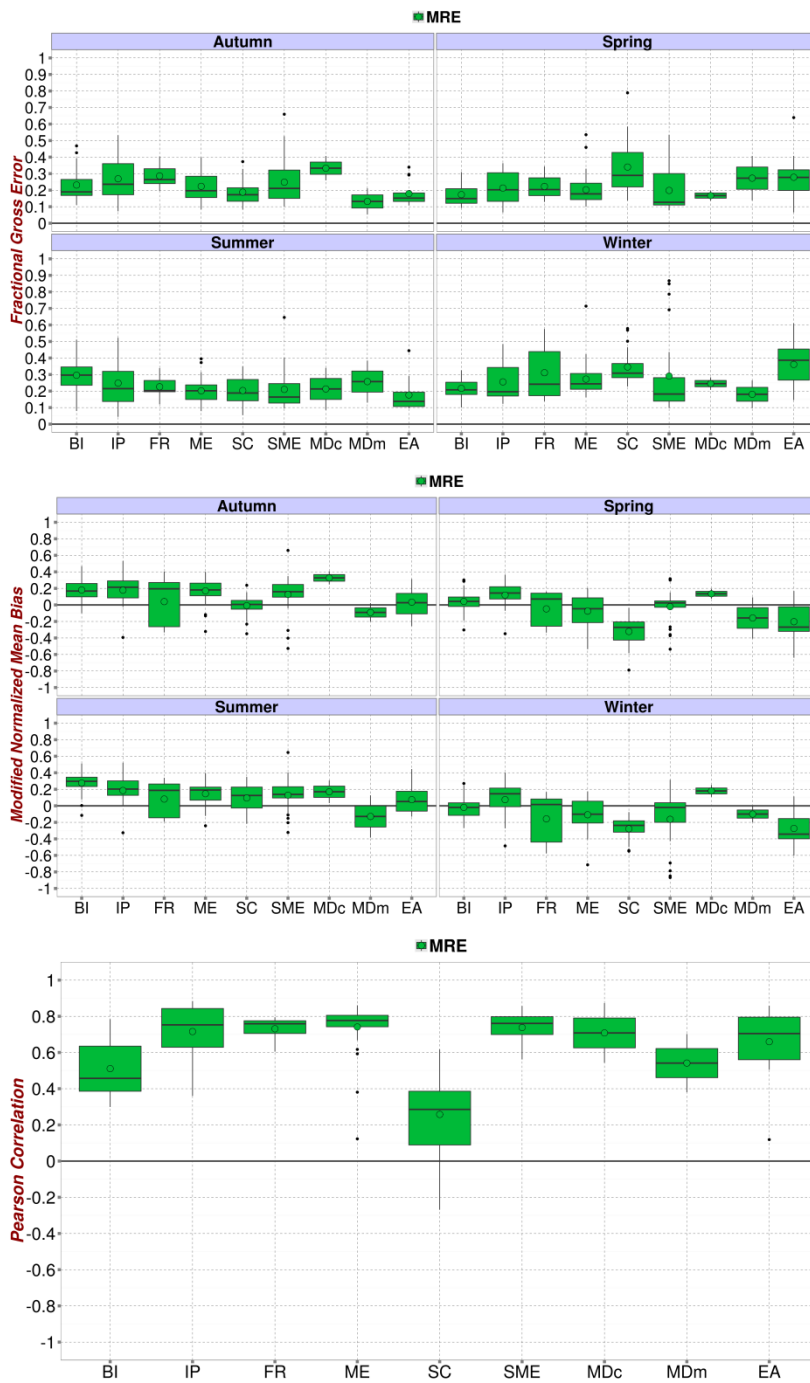
8



1  
 2 Figure 1. The European subregions that were used in the analysis and the corresponding  
 3 EMEP and AIRBASE stations. The numbers denote the number of stations taken into  
 4 consideration for every subregion. The subregions are: the British Isles (BI), France (FR),  
 5 Iberian Peninsula (IP), East Europe (EA), Middle Europe (ME), Mediterranean (MD), South  
 6 Middle Europe (SME) and Scandinavia (SC).

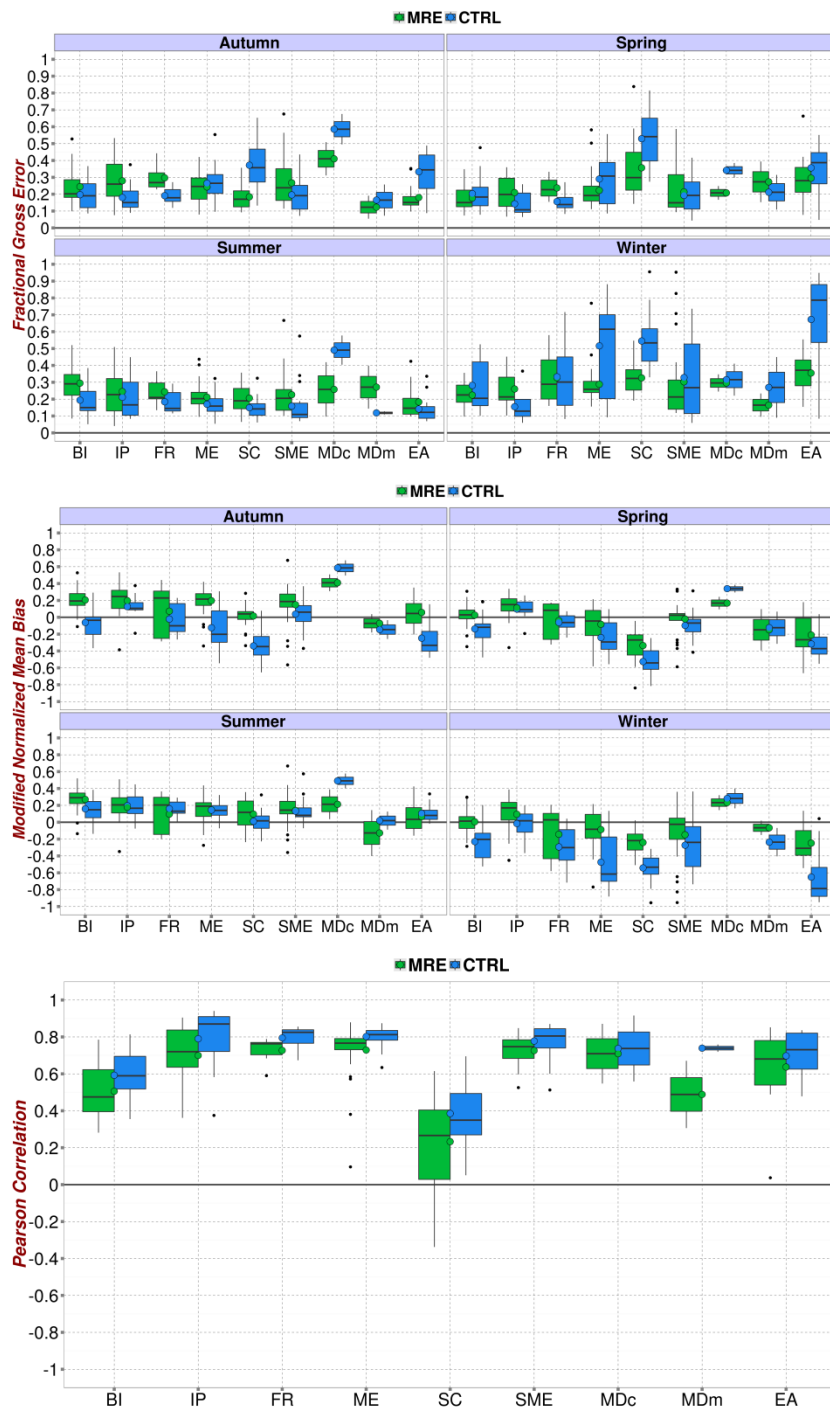
7  
 8

1



2

3 Figure 2. Average 2003-2012 seasonal FGE (top), MNMB (middle) and annual R (bottom) of  
4 near surface ozone for the different European subregions of the MACC reanalysis. The color  
5 dots correspond to means. The bottom and top of the box are the first and third quartiles (Q1  
6 or 25th percentile and Q3 or 75th percentile) and the vertical horizontal line in the box is the  
7 median (Q2 or 50th percentile). The colored points on each box indicate the mean value.



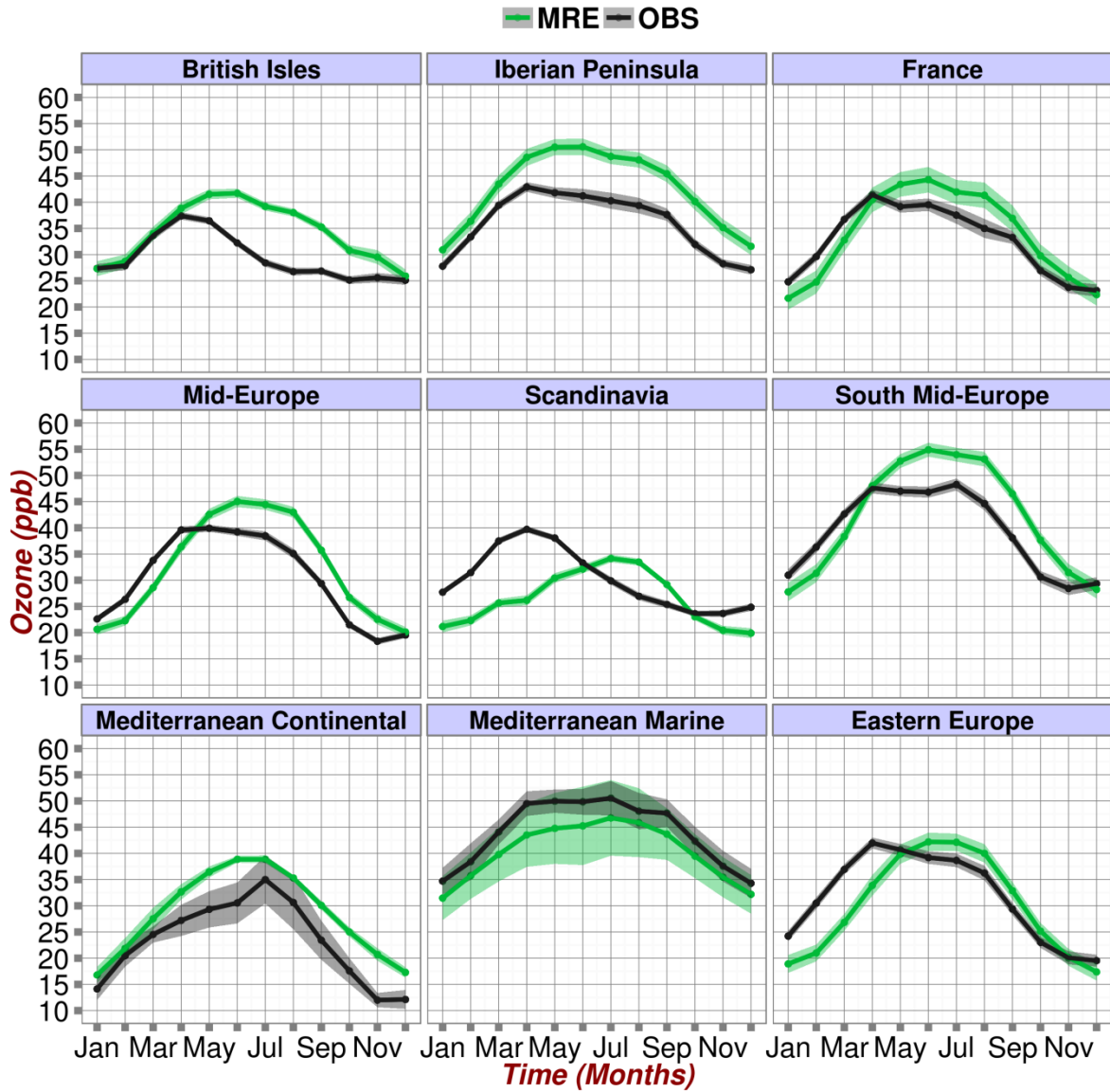
1

2 Figure 3 Average 2003-2010 seasonal FGE (top), MNMB (middle) and annual R (bottom) of  
 3 near surface ozone for the different European subregions of the MACC reanalysis (green) and  
 4 the control run (blue).

5

6

7



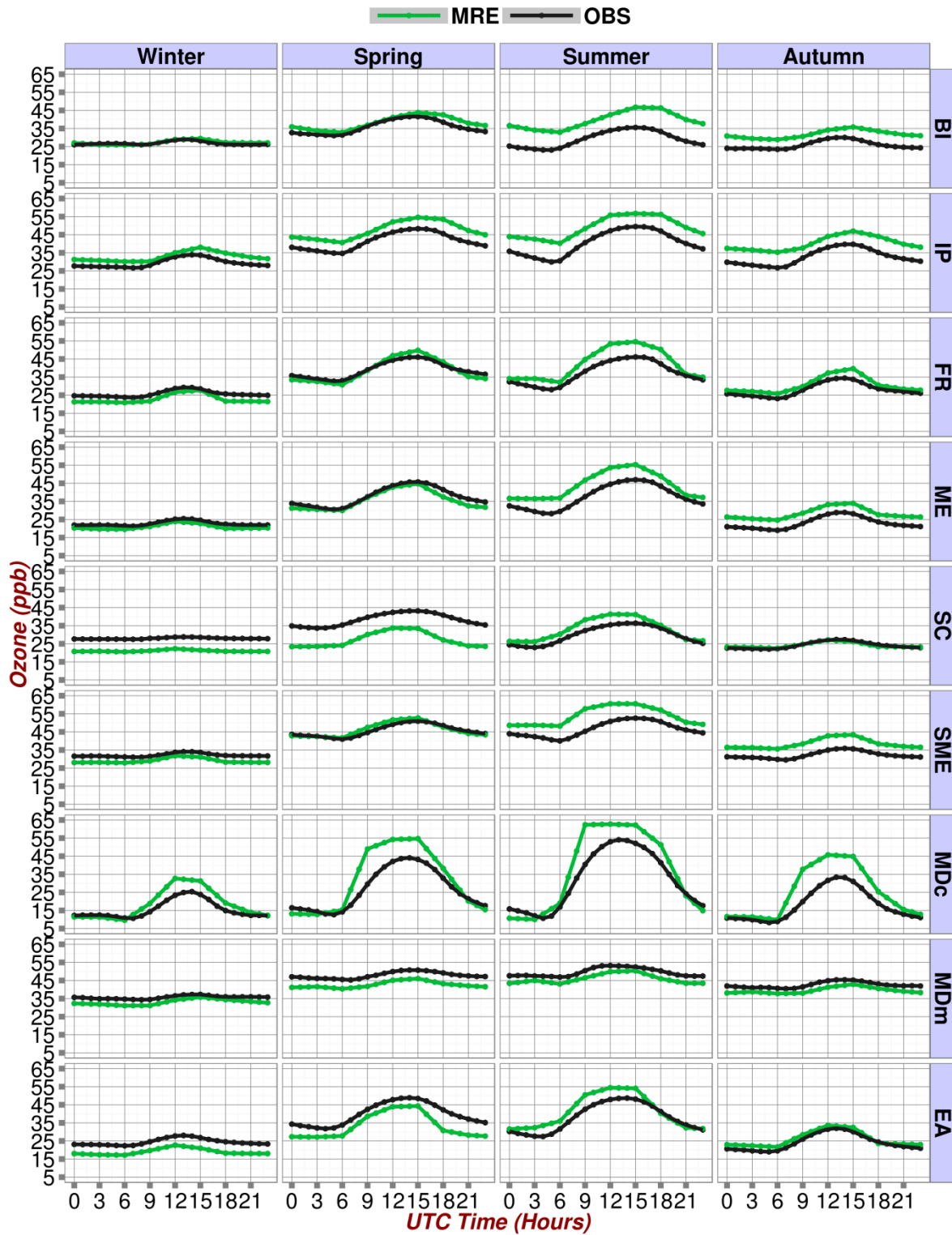
1

2 Figure 4. Mean 2003-2012 annual cycle of near surface ozone for the different European  
 3 subregions of the MACC reanalysis and observations. The shading areas denote 95%  
 4 confidence interval of the mean values.

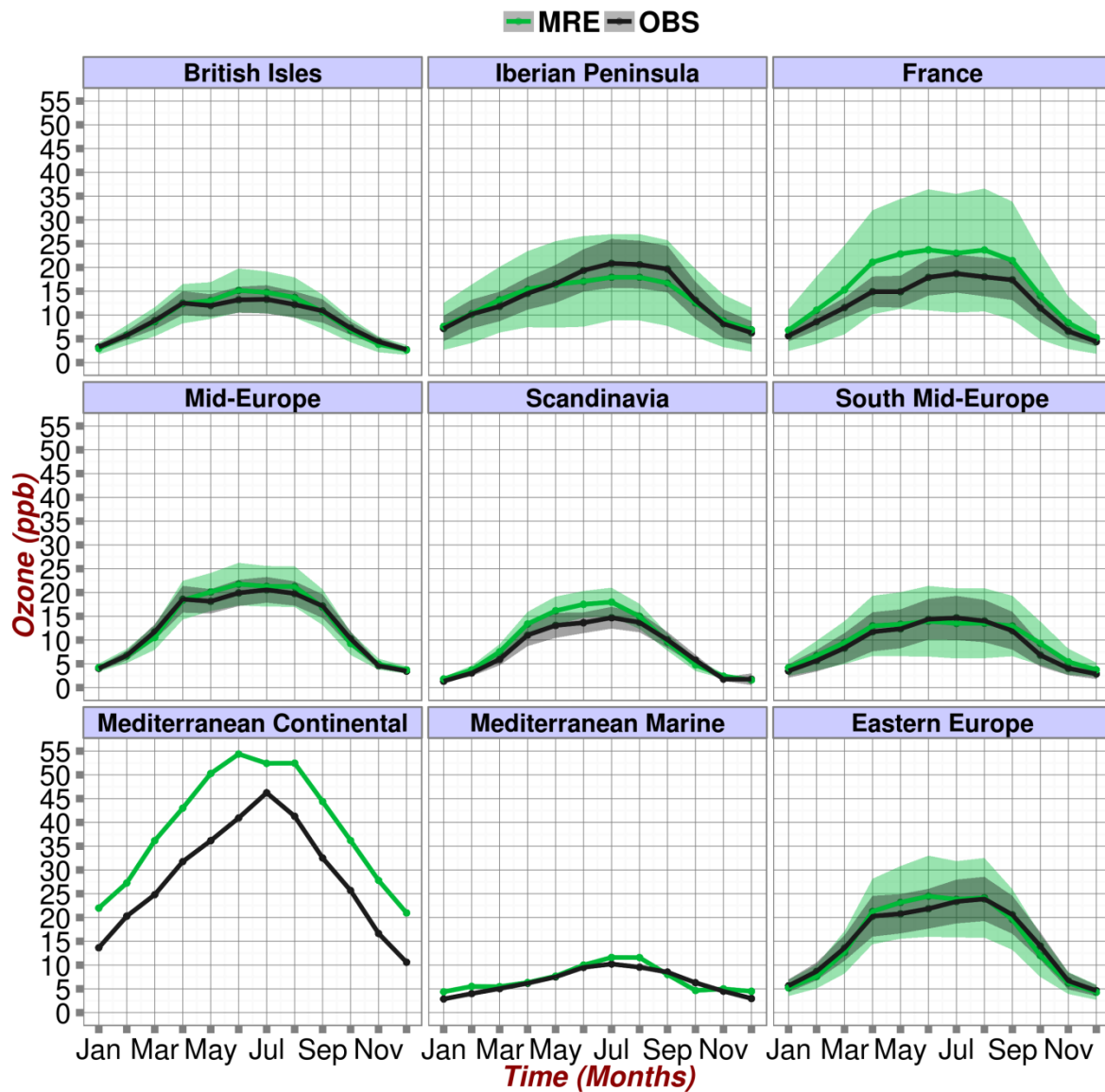
5

6





1  
 2 Figure 5. Mean 2003-2012 diurnal cycle of near surface ozone for the different European  
 3 subregions based on MRE (green line) and observations (black line) calculated for winter  
 4 (DJF), spring (MAM), summer (JJA) and autumn (SON).



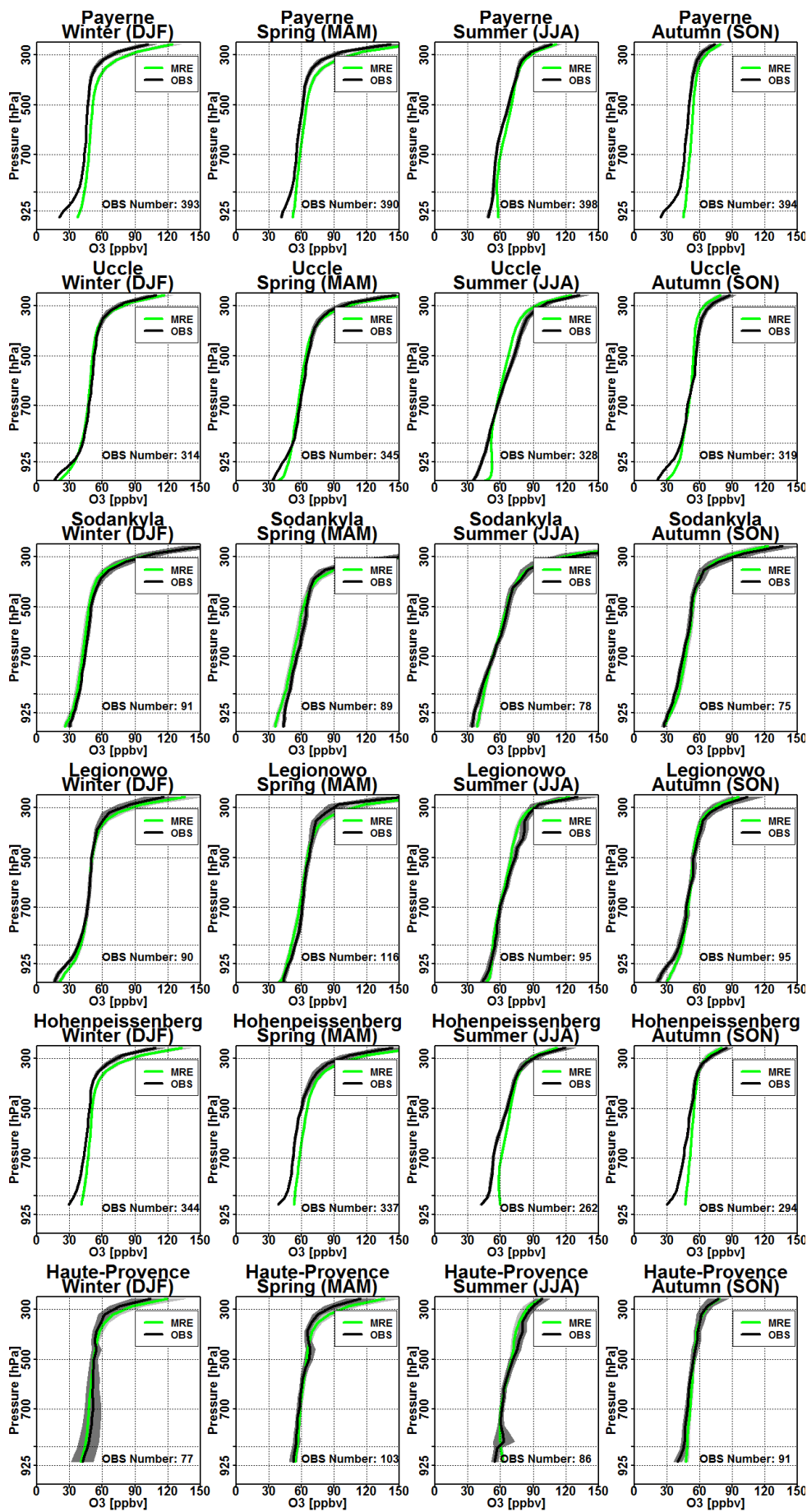
2

3 Figure 6. Annual cycle of the diurnal range of near surface ozone for observations (black  
 4 line) and MRE (green line) averaged over the time period 2003-2012 for the different  
 5 European subregions. Shading areas denote the 95% confidence interval of the mean values.  
 6 The 95% confidence interval is not displayed for the Mediterranean subregions, which  
 7 consist of a limited number of stations.

8

9

10

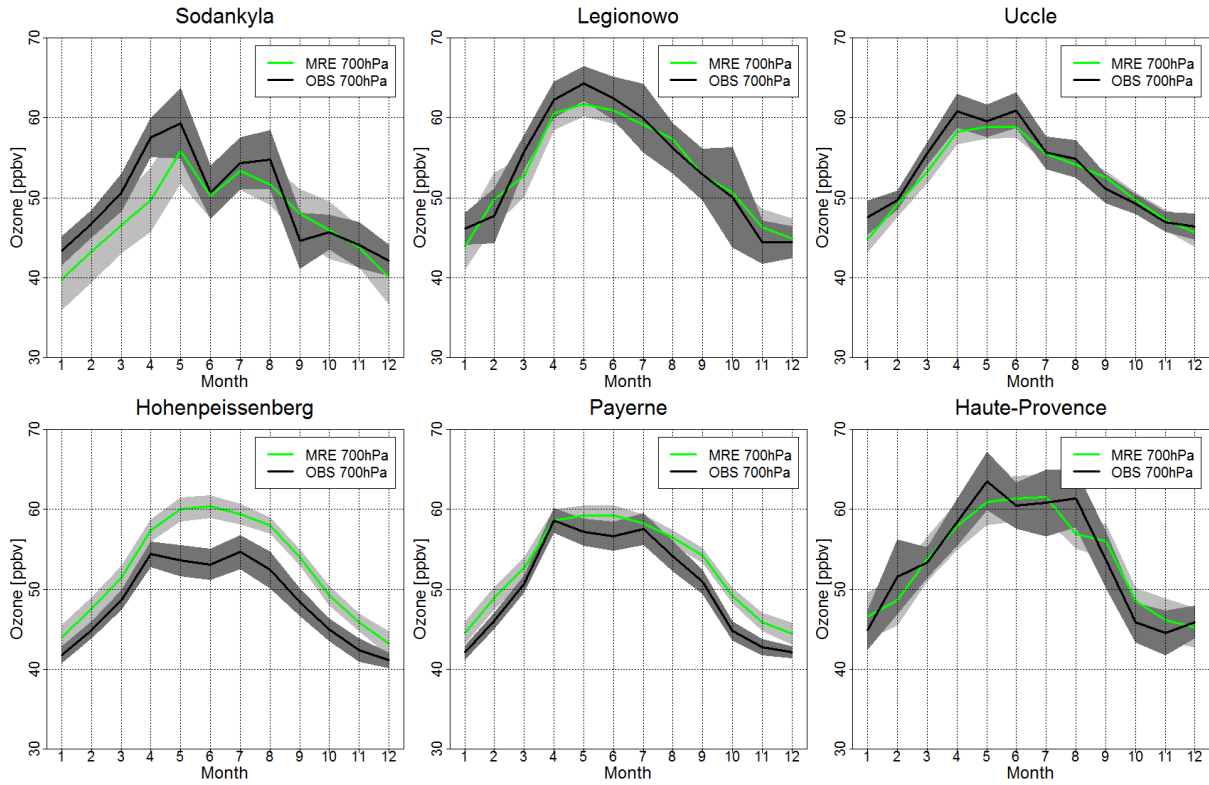


1 Figure 7. Mean 2003-2012 ozone profiles based on MRE near surface ozone (green line) and  
2 ozonesonde measurements (black line) at the stations of Sodankyla (67.4N, 26.6E),  
3 Legionowo (52.4N, 20.9E), Uccle (50.8N, 4.3E), Hohenpeissenberg (47.8N, 11E), Payerne  
4 (46.8N, 6.9E), and Haute-Provence (43.9N, 5.7E). The shading areas denote 95% confidence  
5 interval of the mean values.

6

7

1

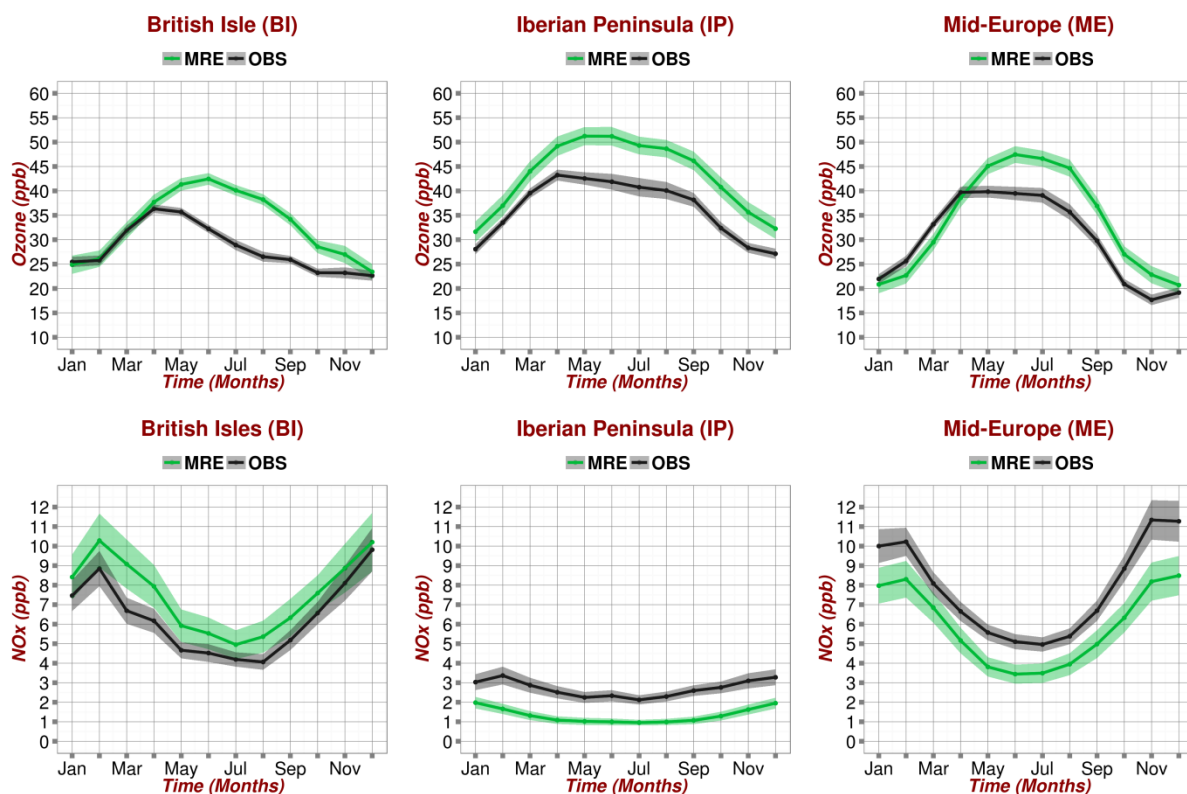


2

3 Figure 8. Mean 2003-2012 annual cycle of lower tropospheric ozone at 700 hPa based on  
4 MRE (green line) and ozonesonde measurements (black line) at the stations of Sodankyla  
5 (67.4N, 26.6E), Legionowo (52.4N, 20.9E), Uccle (50.8N, 4.3E), Hohenpeissenberg (47.8N,  
6 11E), Payerne (46.8N, 6.9E), and Haute-Provence (43.9N, 5.7E). The shading areas denote  
7 95% confidence interval of the mean values.

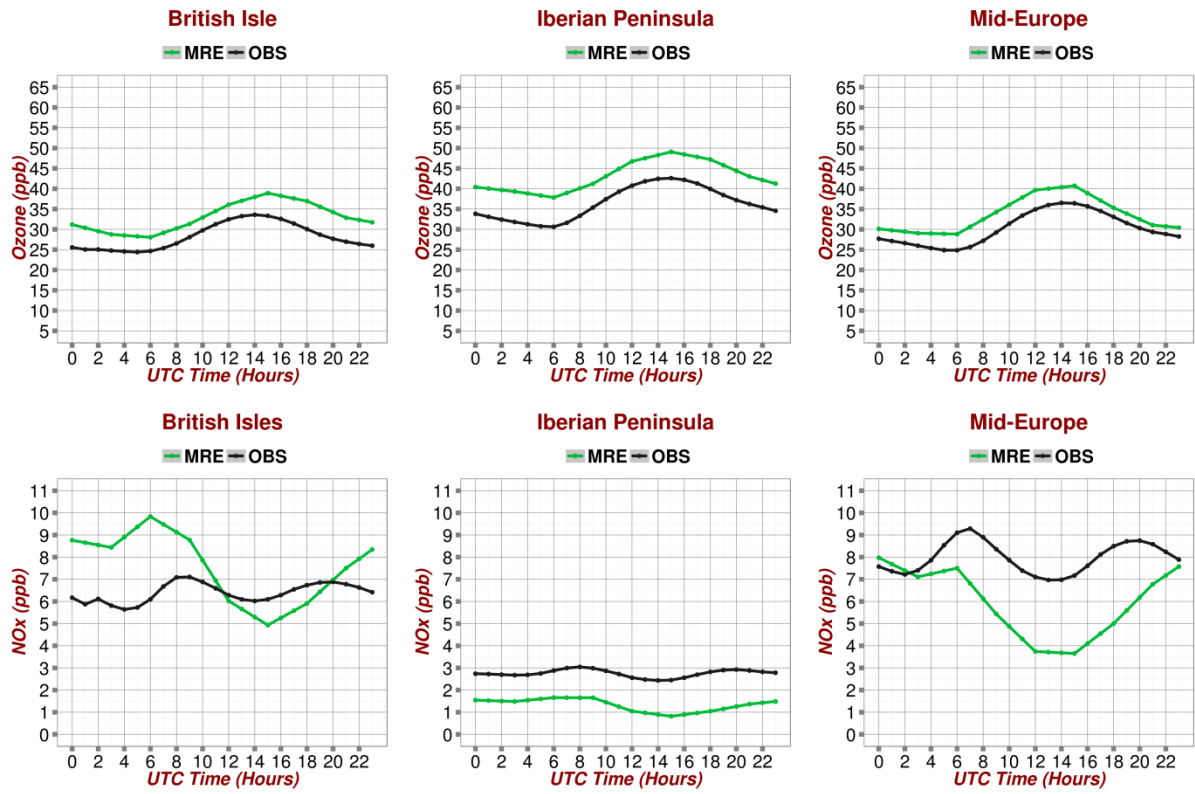
8

1  
2



3  
4  
5  
6  
7

Figure 9. Mean annual cycle of near surface O<sub>3</sub> (top panel) and NO<sub>x</sub> (bottom panel) based on observations (solid black line) and MRE (green line) for the subregions BI, IP, ME over the period 2003-2012.

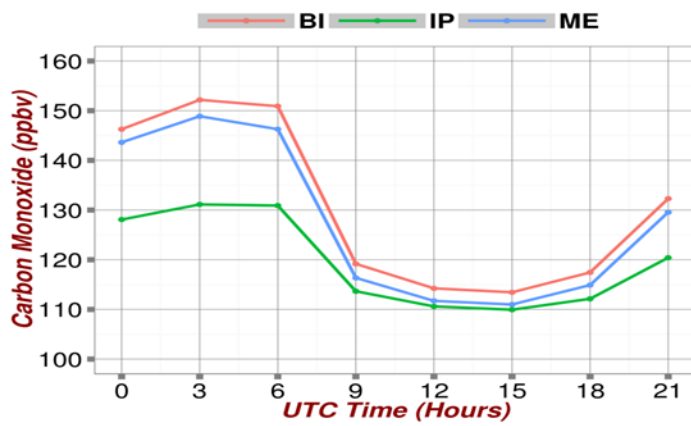
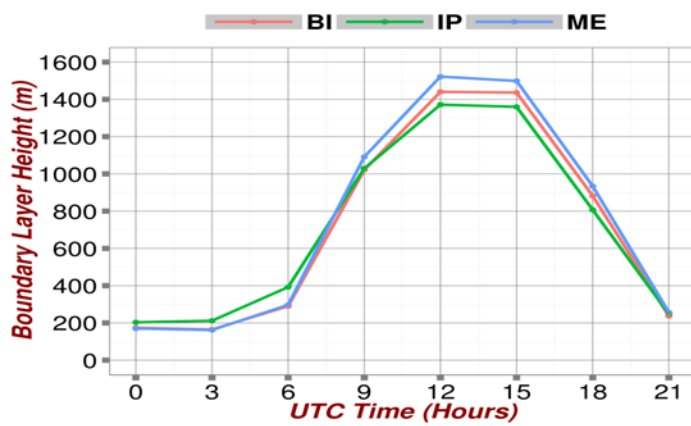
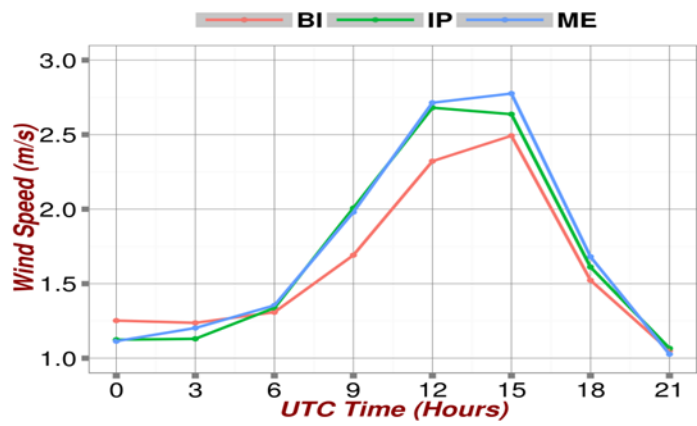


1

2 Figure 10. Mean diurnal cycle of near surface O<sub>3</sub> (top panel) and NO<sub>x</sub> (bottom panel) based  
 3 on observations (solid black line) and MRE (green line) for the subregions BI, IP, ME during  
 4 summer over the period 2003-2012.

5

6



1  
2  
3  
4

Fig S1 Diurnal meteorological patterns of wind speed (upper panel) and boundary layer height (middle panel) and Carbon monoxide (bottom panel).